JPRS L/8879

23 January 1980

USSR Report

PHYSICS AND MATHEMATICS

(FOUO 1/80)

Quantum Electronics

FBIS FOREIGN BROADCAST INFORMATION SERVICE

NOTE

JPRS publications contain information primarily from foreign newspapers, periodicals and books, but also from news agency transmissions and broadcasts. Materials from foreign-language sources are translated; those from English-language sources are transcribed or reprinted, with the original phrasing and other characteristics retained.

Headlines, editorial reports, and material enclosed in brackets [] are supplied by JPRS. Processing indicators such as [Text] or [Excerpt] in the first line of each item, or following the last line of a brief, indicate how the original information was processed. Where no processing indicator is given, the information was summarized or extracted.

Unfamiliar names rendered phonetically or transliterated are enclosed in parentheses. Words or names preceded by a question mark and enclosed in parentheses were not clear in the original but have been supplied as appropriate in context. Other unattributed parenthetical notes within the body of an item originate with the source. Times within items are as given by source.

The contents of this publication in no way represent the policies, views or attitudes of the U.S. Government.

For further information on report content call (703) 351-2938 (economic); 3468 (political, sociological, military); 2726 (life sciences); 2725 (physical sciences).

APPROVED FOR RELEASE: 2007/02/08: CIA-RDP82-00850R000200040048-3

JPRS L/8879

23 January 1980

USSR REPORT

PHYSICS AND MATHEMATICS

(FOUO 1/80)

QUANTUM ELECTRONICS

Moscow KVANTOVAYA ELEKTRONIKA in Russian Vol 6, No 10, 1979
pp 2078-2083, 2097-2108, 2131-2138, 2160-2165, 2195-2198,
2224-2225, 2232-2236, 2245-2248

CONTENTS PAGE

CONTENTS (Continued) Page

UDC 535.416.3

METHOD OF PHASE CONJUGATION IN THE PROBLEM OF COMPENSATING THE THERMAL BLOOMING OF LIGHT BEAMS

Moscow KVANTOVAYA ELEKTRONIKA in Russian Vol 6 No 10, 1979 pp 2078-2083
manuscript received 7 Dec 78

[Article by M.A. Vorontsov, Moscow State University imeni M.V. Lomonosov]

[Text] For the purpose of compensating nonlinear distortions of light beams propagated under conditions of thermal self-stress, an algorithm is suggested for controlling the initial profile of the beam. It is demonstrated that in the linear case the algorithm suggested for optimization by the method of the conditional gradient of the light beam focusing process conforms to the familiar phase conjugation algorithm. The analogy made is employed for the purpose of investigating a number of questions relating to the effectiveness of the operation of phase conjugated adaptive optical systems.

1. Introduction

Light beams propagated in the atmosphere are subject to considerable distortions. These distortions are caused by the effect of a number of factors, among which the greatest influence is exerted by atmospheric turbulence and thermal self-stress, which causes defocusing of the beam. For the purpose of compensating distortions caused by the turbulence of the beam propagation medium are employed adaptive coherent optical technology (KOAT) systems [1]. Adaptive optical systems in existence at the present time are in the form of closed systems for controlling the phase front of the beam and operate on the basis of instantaneous information on the field of the wave reflected from the object. Two key types of KOAT systems are differentiated: phase conjugated and multibeam departing wave [2]. Both types successfully compensate distortions caused by the turbulence of the medium. The major difficulty involves the employment of powerful light beams whose strong thermal self-stress substantially reduces the effectiveness of the operation of KOAT systems [3]. In this connection it is of considerable interest to seek new algorithms suitable for the compensation of nonlinear distortions of light beams.

In this paper the phase conjugation algorithm is generalized for the nonlinear case. It is demonstrated that for beams of low power the phase conjugation algorithm employed in KOAT systems conforms to the algorithm suggested for the optimal focusing of radiation. The analogy made between algorithms makes it possible to investigate the effectiveness of phase conjugation for the purpose of compensating nonlinear distortions of a beam, and also serves as the basis for synthesizing suboptimal algorithms for the focusing of light beams. The method suggested can be used for solving a wide range of problems of optimal control in nonlinear optics.

2. Formulation of Problem

Let us consider a controlled optical system designed for the effective transmission of the energy of a light wave through a nonlinear medium over a certain distance of $z = z_0$. The direction of propagation of the light beam coincides with axis Z^0. At point $z = 0$ is positioned a transmitting optical system forming a train of light pulses of finite duration, t_i, with an initial distribution of the electric field's amplitude of

$$E(x, y, 0, t)=u(x, y, t)\exp\{i\varphi(x, y, t)\}, \tag{1}$$

where $u(x,y,t)$ is the distribution of the field's amplitude within the limits of the transmitting aperture; $\phi(x,y,t)$ is the phase profile of the transmitted pulse. Let us assume that it is possible to form light pulses with arbitrary amplitude, $u(x,y,t)$, and phase, $\phi(x,y,t)$, profiles. The problem of synthesizing a control system consists in constructing a certain algorithm for selecting the initial profile of the beam.

In phase conjugated KOAT systems the amplitude profile of the beam is fixed, and the phase of the transmitted wave, $\phi(x,y,t)$, is set by the reversal in the receiving and transmitting aperture of the phase of the wave reflected from the object. This kind of control algorithm, based on qualitative physical notions, generally speaking is not the best one. For the purpose of constructing an optimal algorithm for controlling the initial profile of the transmitted wave it is necessary to introduce some criterion for optimality of the focusing process. It is most natural to select as this criterion the functional

$$I=\int_0^{t_n} dt \iint_{-\infty}^{\infty} \rho(x, y)\, E(x, y, z_0, t)\, E^*(x, y, z_0, t)\, dxdy, \tag{2}$$

having the sense of the energy of the light wave striking within the limits of the outlet aperture, $\rho(x,y) \geq 0$, during the period of the pulse. For the purpose of simplicity it is assumed that the length of the pulse is great as compared with the time for its propagation to the object. By means of function $\rho(x,y)$ it is possible to take into account different

requirements for the focusing process. For example, if it is necessary to maximize the mean energy density of the pulse at point x_0,y_0 in the object, then $\rho(x,y) = \delta(x - x_0, y - y_0)$, where $\delta(x,y)$ is a delta function. In focusing the beam on area S of the object, $\rho(x,y) = 1$ everywhere inside of S , and $\rho(x,y) = 0$ outside of this area. The problem of optimizing the process of focusing light pulses can be formulated in the following manner: It is necessary to synthesize an algorithm for controlling the phase of the beam, $\phi(x,y,t)$, and the amplitude profile, $u(x,y,t)$, which will enable maximization of the focusing functional (2). The finite value of the energy of the transmitted pulse, W_0 , imposes a limitation on selection of the beam's amplitude profile.

We will assume that the light pulse is propagated in a nonlinear slightly absorbent medium moving in the direction of axis X . The change in the complex amplitude of the wave's electric field, $E(x,y,z,t)$, is described by the quasi-optics equation [4]

$$2ik\frac{\partial E}{\partial z} = \Delta_\perp E + k^2\tilde{\varepsilon}E + RTE \tag{3}$$

and by the matter equation

$$\frac{\partial T}{\partial t} + \theta_x\frac{\partial T}{\partial x} = \theta_\chi\Delta_\perp T + EE^*, \tag{4}$$

the form of which is determined by the heat transfer mechanism. System of equations (3) and (4) is written in the accompanying system of coordinates: Here k is the wave number, $\tilde{\varepsilon}$ represents fluctuations in the dielectric constant caused by irregular inhomogeneities and by heating of the medium from preceding pulses, and R is the nonlinearity parameter. Negative parameters θ_x and θ_χ in heat conduction equation (4) are determined via the density of the medium, its heat conduction and the rate of movement along axis X .

3. Optimal Focusing Algorithm

We will maximize functional (2) by employing the gradient method of optimization in [5]. As applied to the problem considered, the essence of this method reduces to the following [6]. Sought is the main linear portion, ΔI , of the increment in the focusing functional caused by some change in the initial profile of the beam, $E(x,y,0,t)$. From (2) it follows that

$$\delta I = 2\mathrm{Re} \int_0^{t_н} dt \iint_{-\infty}^{\infty} \rho(x,y) E^*(x,y,z_0,t)\, \Delta E(x,y,z_0,t)\, dxdy. \tag{5}$$

In order to evaluate the influence of an increment in the initial profile on the change in the value of functional I , it is necessary to arrive at the dependence of δI on increment ΔE at point $z = 0$, and not at point $z = z_0$, as in equation (5). This can be done by employing the following representation of equation (5):

$$\delta I = 2\mathrm{Re} \int_0^{z_0} dz \int_0^{t_н} dt \iint_{-\infty}^{\infty} \frac{\partial(\psi \Delta E)}{\partial z} dxdy + 2\mathrm{Re} \int_0^{t_н} dt \iint_{-\infty}^{\infty} \psi(x,y,0,t) \times \\ \times \Delta E(x,y,0,t)\, dxdy, \tag{6}$$

where $\psi(x,y,z,t)$ is an adjoint function satisfying boundary condition

$$\psi(x, y, z_0, t) = \rho(x, y) E^*(x, y, z_0, t). \tag{7}$$

The second term in (5) describes the dependence sought of δI on $\Delta E(x,y,0,t)$. In the appendix it is demonstrated that the first term in (6) can be equated to zero, by imposing on function $\psi(x,y,z,t)$ the following limitations:

$$-2ik \frac{\partial \psi}{\partial z} = \Delta_\perp \psi + k^2 \tilde{\varepsilon} \psi + RT\psi + 2iRE^*G, \tag{8}$$

$$-\frac{\partial G}{\partial t} - \theta_x \frac{\partial G}{\partial x} = \theta_x \Delta_\perp G + \mathrm{Im}(E\psi),\ G(x,y,z,t_н) = 0. \tag{9}$$

The physical interpretation of adjoint system of equations (8) and (9) is discussed in sec 4. It is easy to express increment $\Delta E(x,y,0,t)$ in terms of the corresponding increments in the amplitude, $\Delta u(x,y,t)$, and phase, $\Delta\phi(x,y,t)$, profiles: $\Delta E(x,y,0,t) = \exp(i\phi)\Delta u + iu \exp(i\phi)\Delta\phi$. Substituting this expression in (6), we finally get

$$\delta I = \int_0^{t_н} dt \iint_{-\infty}^{\infty} (I'_u \Delta u + I'_\varphi \Delta\varphi)\, dxdy, \tag{10}$$

where $I'_u = 2|\psi(x,y,0,t)| \cos(\phi+\eta)$; $I'_\phi = -2u(x,y,t)|\psi(x,y,0,t)| \sin \sin(\phi+\eta)$ are gradients of functional I ; $\eta = \eta(x,y,t) = \arg \psi(x,y,0,t)$.

Having expressions for gradients I'_u and I'_ϕ, it is possible to write an algorithm for correcting the initial profile of the transmitted wave:

$$u_{n+1}(x, y, t)=u_n(x, y, t)+\beta I'_u, \quad n=0, 1, 2, \ldots \tag{11}$$

where β is a certain factor of the gradient method taking into account the limitation on the total energy of the pulse, $\phi_{n+1}(x,y,t) = \phi_n(x,y,t) + \gamma I'_\phi$, where $n = 0, 1, 2, \ldots$. For the purpose of correcting the phase front it is most convenient to employ the method of the conditional gradient [5], according to which the following, the $n + 1$-th, approximation of the phase is determined from the condition $\max(\delta I)$ in terms of ϕ. The maximum in (10) is achieved with $\phi(x,y,t) = -\eta(x,y,t)$ and

$$\varphi_{n+1}(x, y, t)=\varphi_n(x, y, t)-\alpha[\varphi_n(x, y, t)+\arg\psi(x, y, 0, t)], \tag{12}$$

where $0 \leq \alpha \leq 1$ is the coefficient of the gradient method. With $\alpha = 1$ the iteration procedure for correcting the phase profile reduces to the successive conjugation of the phase at point $z = 0$ of function $\psi(x,y,0,t)$.

From the analysis made it follows that for the next, $n + 1$-th, change in the initial profile of the transmitted wave it is necessary first to solve boundary problem (3), (4) from $z = 0$ to $z = z_0$ with the initial distribution of the field within the limits of the transmitting aperture, $E(x,y,0,t) = u_n(x,y,t) \times \exp[i\phi_n(x,y,t)]$, and secondly to solve adjoint boundary condition (8), (9) with the boundary condition in (7) from $z = z_0$ to $z = 0$, and, employing the function found, $\psi(x,y,0,t)$, to calculate the next approximation of the initial amplitude profile according to (11) and of the phase profile according to the phase conjugation algorithm for function $\psi(x,y,0,t)$ (12).

The optimal focusing algorithm was tested in a steady-state problem regarding the propagation of a light beam in a moving regular medium. With sufficiently high speeds of the medium, the dimensionless equations describing the propagation of the light beam have the form

$$2i\frac{\partial E}{\partial z}=\Delta_\perp E+RTE;\ \frac{\partial T}{\partial x}=EE^*,$$

where variables x and y are normalized for the initial radius of the beam, and z for the diffraction length; the amplitude of the field relates to the absolute value of the amplitude maximum with $z = 0$. By means of the algorithm described was optimized the power of the light wave within the limits of an outlet aperture, $\rho(x,y) = \exp[-(x^2 + y^2)]$, positioned at half the diffraction length. Beams were considered with a Gaussian amplitude profile, $u(x,y) = \exp[-(x^2 + y^2)/2]$, which did not vary. Some results of optimization of the phase profile of the radiated wave, obtained with different values of nonlinear parameter R, are presented in the table.

Table

R	—14	—20	—28
I_0	1,4	1,2	0,75
I_k	0,8	0,6	0,5

The values of focusing criterion I_0, calculated according to the optimal focusing algorithm suggested, are given in the second line of the table. For comparison, in the bottom line are indicated the corresponding values of criterion I_k arrived at according to the method suggested in [7] for phase compensation of nonlinear distortions. The results of the calculations made testify to the effectiveness of employing the gradient method for optimizing the initial profile of the beam.

4. Optimal Focusing and Phase Conjugation

Let us discuss the relationship between the optimal focusing algorithm suggested and the phase conjugation algorithm. Let us consider the linear case when thermal self-stress of the light pulse can be disregarded (parameter R in equations (3) and (8) equals zero). Adjoint equation (8) in this case has a distinct physical meaning: It describes the propagation of the wave from the object, $z = z_0$, to the transmitting and receiving aperture, $z = 0$. Boundary condition (7) denotes conjugation at point $z = z_0$ of the phase of the wave striking the object, whereby function $\rho(x,y)$ can be interpreted as the peak reflection coefficient of the surface. If $\rho(x,y) = \delta(x - x_0, y - y_0)$, then boundary condition (7) describes the reflection of the transmitted wave from point (x_0,y_0,z_0) and adjoint function $\psi(x,y,z,t)$ has the meaning of the complex amplitude of the wave reflected from a point object. In this case the phase correction algorithm in the form of (12) with $\alpha = 1$ denotes the reversal in the receiving and transmitting aperture of the wave front of the reflected wave.

Thus, it has been demonstrated that a phase conjugated KOAT system operating in a linear medium in relation to a point object practically realizes the algorithm suggested for optimization of the focusing functional by the conditional gradient method. The analogy drawn between the optimal focusing and phase conjugation algorithms makes it possible to reduce the analysis of the latter to an investigation of the iteration procedure for optimization of the quadratic functional by the gradient method. This approach can prove to be quite useful. For example, based on the comparison of algorithms made it is possible to suggest for KOAT systems an algorithm different from the usual phase conjugation. Actually, the conditional

gradient method with $\alpha = 1$, which is realized in KOAT systems, is generally speaking rather crude. For the purpose of improving convergence of the iteration process, coefficient α must be reduced in proportion to convergence of the algorithm. Such an algorithm in the form of (12) with the fine subdivision of α and the storage of the phase of the transmitted wave can be realized with modern high-speed KOAT systems capable of making several corrections of the phase front during the period of "freezing" of the medium's turbulence.

The algorithms discussed for correction of the phase of the transmitted wave cease to be identical in cases when the reflecting surface of the object does not have an isolated shiny point or the beam propagation medium is nonlinear.

In the first case boundary condition (7) for the adjoint function does not agree with the condition for reflection of the transmitted wave, which we write in the following form:

$$\psi_0(x, y, z_0, t)=\rho(x, y) \exp [i \xi(x, y)]E(x, y, z_0, t), \quad (13)$$

where $\psi_0(x,y,z,t)$ is the complex amplitude of the field of the wave reflected from the object with a reflection coefficient of $\rho(x,y)$ exp exp $[i\xi(x,y)]$. The difference is associated with the change in the phase profile of the wave in reflection from the rough surface of the object; in addition, condition (7) assumes conjugation of the wave's phase at point $z = z_0$. From the viewpoint of effectiveness of the transmission of the light wave's energy over assigned distance z_0, boundary condition (7) is preferable to reflection condition (13). Acutally, with condition (7) the return wave is propagated along an optical path closer to the optical path of the radiated wave (with $\rho(x,y) = 1$ they agree), than is the reflected wave, and consequently phase distortions can be more accurately compensated by reversal of the wave front of this wave. In this connection, one of the methods for improving the effectiveness of the transmission of light energy can be the practical realization of boundary condition (7) as the result of installing on the exposed object (if this is possible) a phase conjugation device. Another reason for reduction of the effectiveness of phase conjugation is the nonlinearity of the beam propagation medium. In this case adjoint system of equations (8), (9) does not describe the wave reflected from the object and consequently the phase conjugation algorithm does not optimize focusing functional (2).

Appendix

Let us demonstrate that in the fulfillment of conditions (7) to (9) imposed on adjoint functions ψ and G expression

$$s = 2\mathrm{Re}\int_0^{z_0} dz \int_0^{t_M} dt \iint_{-\infty}^{\infty} \left[\frac{\partial\psi}{\partial z}\Delta E + \psi\frac{\partial \Delta E}{\partial z}\right] dxdy$$

equals zero. From equations (3) and (4) it is easy to arrive at equations for derivatives $\partial\Delta E/\partial z$ and $\partial\Delta T/\partial z$:

$$\frac{\partial \Delta E}{\partial z} = \frac{1}{2ik}\left[\Delta_\perp(\Delta E) + k^2\tilde{\varepsilon}\Delta E + RT\Delta E + RE\Delta T\right], \tag{14}$$

$$\frac{\partial \Delta T}{\partial z} + \theta_x\frac{\partial \Delta T}{\partial x} - \theta_\chi\Delta_\perp(\Delta T) - 2\mathrm{Re}\,(E^*\Delta E) = 0. \tag{15}$$

Substituting (14) in s and integrating by parts the term with $\Delta_\perp(\Delta E)$, we get

$$s = \frac{1}{k}\mathrm{Im}\int_0^{z_0} dz \int_0^{t_M} dt \iint_{-\infty}^{\infty}\left[\Delta E\left(2ik\frac{\partial\psi}{\partial z} + \Delta_\perp\psi + k^2\tilde{\varepsilon}\tilde{\psi} + RT\psi\right) + \Delta T RE\psi\right] dxdy.$$

Multiplying equality (15) by $G(x,y,z,t)R/k$, and integrating in terms of variables z, t, x, and y, we have

$$\frac{R}{k}\int_0^{z_0}\int_0^{t_M} dzdt \iint_{-\infty}^{\infty}\left[\left(-\frac{\partial G}{\partial t} - \theta_x\frac{\partial G}{\partial x} - \theta_\chi\Delta_\perp G\right)\Delta T + 2\,\mathrm{Im}\,(iGE^*\Delta E)\right] dxdy = 0.$$

Subtracting this expression from s, we finally get

$$s = \int_0^{z_0} dz \int_0^{t_M} dt \iint_{-\infty}^{\infty}\left\{\frac{R}{k}\left[\frac{\partial G}{\partial t} + \theta_x\frac{\partial G}{\partial x} + \theta_\chi\Delta_\perp G + \mathrm{Im}\,(E\psi)\right]\Delta T + \right.$$
$$\left. + \frac{1}{k}\mathrm{Im}\left[2ik\frac{\partial\psi}{\partial z} + \Delta_\perp\psi + k^2\tilde{\varepsilon}\tilde{\psi} + RT\psi + 2iGE^*\right]\Delta E\right\} dxdy.$$

According to (8), (9), expressions with ΔT and ΔE equal zero, i.e., $s = 0$, Q.E.D.

The method presented above for arriving at an adjoint system of equations it is not complicated to extend to a system of quasi-optical equations describing the diffraction of waves in nonlinear media [8], as well as to matter equations of a more complex type, e.g., $LT = f(p)$, $p = EE^*$, where L is the linear differential operator and $f(p)$ is a certain intensity function. In this case the adjoint equation for function G will have the form $\overline{L}G = (df/dp)\,\mathrm{Im}\,(E\psi)$, where $\overline{L}$ is the adjoint operator of L .

Bibliography

1. Bakut, P.A., Ustinov, N.D., Troitskiy, I.N. and Sviridov, K.N. ZARUBEZHNAYA RADIOELEKTRONIKA, No 3, 55 (1977).

2. Khardi, Dzh.U. TRUDY IIER, 66, No 6, 31 (1978).

3. Herrman, J. J. OPT. SOC. AMER., 65, 1212 (1975).

4. Akhmanov, S.A., Krindach, D.P., Migulin, A.V., Sukhorukov, A.P. and Khokhlov, R.V. IEEE J., QE-4, 568 (1968).

5. Vasil'yev, F.P. "Lektsii po metodam resheniya ekstremal'nykh zadach" [Lectures on Methods of Solving Extremum Problems], Moscow, MGU, 1974.

6. Vorontsov, M.A. "Tezisy dokladov I Vsesoyuz. konf. 'Problemy upravleniya parametrami lazernogo izlucheniya'" [Theses of Papers at the First All-Union Conference "Problems in Controlling the Parameters of Laser Radiation"], Tashkent, 1978, Part II, p 157.

7. Yegorov, K.D. and Kandidov, V.P. "Tezisy dokladov I Vsesoyuz. konf. 'Problemy upravleniya parametrami lazernogo izlucheniya,'" Tashkent, Part I, 1978, p 170.

8. Karamzin, Yu.N., Sukhorukov, A.P., Sukhorukova, A.K. and Chernega, P.I. DAN SSSR, 235, 564 (1977).

CSO: 1862
8831

UDC 621.391.837:621.373.826

IMAGE OF A DIFFUSE OBJECT IN A RANDOMLY INHOMOGENEOUS MEDIUM WITH AMPLITUDE DISTORTIONS

Moscow KVANTOVAYA ELEKTRONIKA in Russian Vol 6 No 10, 1979 pp 2097-2102
manuscript received 16 Jan 79

[Article by P.A. Bakut, V.V. Barinov, N.A. Dimov, V.I. Mandrosov, A.S. Pechenov and I.N. Troitskiy]

[Text] The influence is discussed of amplitude distortions on the distribution of intensity in the image of a diffuse object produced in a randomly inhomogeneous medium on the assumption that the logarithm of amplitude distortions is distributed normally. It is demonstrated that distortions in this distribution depend substantially on parameter $\eta = \rho_a^2\sigma^2/S$ (where ρ_a and σ are the correlation radius and variance of the logarithm of amplitude distortions and S is the area of the receiving aperture), as well as on the resolution of the receiving equipment. The conclusion is confirmed experimentally.

It is known that in the propagation of radiation scattered by an object through a randomly inhomogeneous medium fluctuations arise in this radiation which result in its focusing in the formation of a distorted image of the object [1]. In this connection the problem arises of improving the quality of the image produced under such conditions. In recent times more and more attention has been devoted to the question of producing an undistorted image of the object by means of the compensation of phase fluctuations in the field of the wave originating in the propagation of radiation from this object in a randomly inhomogeneous medium. Here it is usually assumed that uncompensated amplitude distortions do not have an important influence on image quality [1].

The purpose of this study is to show that conditions exist under which it is impossible to disregard the influence of amplitude fluctuations which arise in the propagation of radiation in a randomly inhomogeneous medium, on the distribution of intensity in the image. Let us consider the field in the image of a diffuse object. It is not difficult to demonstrate that with the total compensation of phase distortions and with the object placed in a region where amplitude distortions are isoplanar, the field in the image can be represented in the form

$$E(\delta) = \frac{ik^2}{Rf} \int E_0(r)\, h_\alpha \left[\frac{k}{2}\left(\frac{r}{R} + \frac{\delta}{f}\right)\right] dr, \tag{1}$$

where r and δ are the radius vectors of the object and receiving aperture; f is the focal length of the receiving system; R is the distance to the object; $h_\alpha(z) = S^{-1} \exp[\alpha(\rho) + iz\rho]d\rho$ is the pulse response taking amplitude distortions into account; S is the area of the receiving aperture; $k = 2\pi/\lambda$ is the wave vector; λ is the wavelength of radiation from the object; $\alpha(\rho)$ is the logarithm of amplitude distortions; $E_0(r)$ is the distribution of the field scattered by the object over its surface. Let us assume that $E_0(r)$ and $\alpha(\rho)$ are distributed normally with correlation functions of:

$$\overline{E_0(r_1)\, E_0^*(r_2)} = u(r_1)\, \delta(r_1 - r_2), \tag{2}$$

$$\langle \alpha(\rho_1)\alpha(\rho_2)\rangle = \sigma^2 \exp[-(\rho_1-\rho_2)^2/\rho_a^2], \tag{3}$$

where ρ_a is the correlation radius of the logarithm of amplitude distortions; $\sigma^2 = \langle\alpha^2\rangle - \langle\alpha\rangle^2$; $u(r)$ is the distribution of intensity over the surface of the object; and the line above the product $E_0(r_1)E^*_0(r_2)$ indicates averaging for different realizations of the diffuse object, and the angle brackets, averaging for different realizations of amplitude fluctuations.

The assumption regarding the normal distribution of $E_0(r)$ was confirmed experimentally in [2]; the assumption regarding the normality of the distribution of $\alpha(\rho)$, as can be concluded from [3], is fulfilled approximately in the range of $0 < \sigma < 2$. Then, employing the law of the conservation of intensity in [3], which results in the fact that $\langle\exp[2\alpha(\rho)]\rangle = 1$, as well as the equation

$$\langle \exp[\alpha(\rho_1) + \alpha(\rho_2)]\rangle = \exp[-2(\sigma^2 - \langle\alpha(\rho_1)\alpha(\rho_2)\rangle)], \tag{4}$$

we get with an accuracy of an insignificant constant factor the mean distribution of intensity in the image:

$$I(\delta) = \langle|\overline{E(\delta)}|^2\rangle = \frac{k^2S^2}{R^2f^2} \int u(r)\left\langle \left| h_\alpha\left[\frac{k}{2}\left(\frac{r}{R} + \frac{\delta}{f}\right)\right]\right|^2\right\rangle dr. \tag{5}$$

We will make a further analysis for the conditions usually fulfilled in practice, $\rho_a^2 \ll S$ and $\sigma^2\rho_a^2/S \ll 1$. Then

$$I(\delta)=I_0(\delta)+I_1(\delta);$$
$$I_0(\delta)=\frac{k^4S^2}{R^2f^2}\int u(\mathbf{r})\left|h_0\left[\frac{k}{2}\left(\frac{\mathbf{r}}{R}+\frac{\delta}{f}\right)\right]\right|^2 d\mathbf{r};$$
$$I_1(\delta)=\frac{k^4S^2}{R^2f^2}\rho_a^2\sigma^2\int u(\mathbf{r})\exp\left[-\frac{k^2\rho_a^2}{4}\left(\frac{\mathbf{r}}{R}+\frac{\delta}{f}\right)^2\right]d\mathbf{r}, \tag{6}$$

where $h_0(z) = S^{-1}\int \exp(iz\rho)d\rho$ is the pulse response of the optical system in the total absence of fluctuations. Below we will consider the case of most interest for practice, that of sufficiently good angular resolution, when the object has sufficient dimension. In this case the image produced at a single wavelength consists on average of $M = SS_0/(\lambda^2R)$ spots [2], whereby $M \gg 1$. Then it is not difficult to demonstrate that

$$I_0(\delta)=\lambda^2R^2u(\mathbf{r}),\quad \mathbf{r}=R\delta/f; \tag{7}$$

$$I_1(\delta)=\rho_a^2S\sigma^2\int u(\mathbf{r})\exp\left[-\tfrac{1}{4}k^2\rho_a^2(\mathbf{r}/R+\delta/f)^2\right]d\mathbf{r}, \tag{8}$$

where S_0 is the area of the object.

Let us then consider three of the most typical cases, when the analytical expression for $I_1(\delta)$ is of the most simple form.

First case: $M \ll S/\rho_a^2$. Here function $u(\mathbf{r})$ is narrower in terms of $\mathbf{r}$ than function $\exp[-(1/4)k\rho_a^2(\mathbf{r}/R + \delta/f)^2]$, and

$$I_1(\delta)=S\rho_a^2\sigma^2\int u(\mathbf{r})\exp\left[-k^2\rho_a^2\delta^2/(4f^2)\right]d\mathbf{r}. \tag{9}$$

In this case $I_1(\delta)$ represents the background with a maximum at $\delta = 0$ and with an intensity distribution which drops smoothly toward the edges. This background, superposed on the image, can distort it; the degree of distortion is characterized by parameter $\eta = I_1(0)/I_0(0)$. Let us estimate it for objects with a uniform distribution of intensity of $u(\mathbf{r}) = \text{const} = u_0$. Then

$$\eta=M\rho_a^2\sigma/S. \tag{10}$$

If $\eta \geq 0.3$, i.e., $M \geq S/(3\rho_a^2\sigma^2)$, then distortions of the image resulting from amplitude fluctuations are great. When $\eta \leq 0.1$, i.e., with $M \leq S/(10\rho_a^2\sigma^2)$, these distortions are relatively slight, which is associated with the triviality of ρ_a with the condition $1 \ll M \ll S/\rho_a^2$.

This results in the formation around each spot forming the image of a background greater in width than the dimensions of the image. In proportion to an increase in the number of spots, M , in the image, the background from each spot is superposed on the image, at the same time worsening its quality.

The second case: $M \gg S/\rho_a^2$. Here function $u(r)$ is broader than function $\exp\left[-(1/4)k^2\rho_a^2(r/R \mp \delta/f)^2\right]$, and

$$I_1(\delta)=R^2\sigma^2\lambda^2 u(r); \quad r=R\delta/f, \tag{11}$$

i.e., the image is practically not distorted.

Finally, let us consider the case when $1 \ll M \leq 5S/\rho_a^2$; $S/\rho_a^2 \geq 10$. In each specific realization of $I(\delta)$ each spot which would be present in the absence of distortions, without changing its position is transformed into a number of spots of less intensity, and the region occupied by a single spot so transformed is of a size comparable with the size of the image itself. For the purpose of proving these statements, let us imagine that the image of a diffuse object consists of a combination of images of M independent plane waves. This assumption, as is obvious from [2], is totally justified. The averaged distribution of intensity in each of these images, $I_n(\delta)$, is arrived at by the substitution of $u_n(r) = \delta(r - r_n)$ in equation (8):

$$I_n(\delta)=\exp\left[-{}^1/_4 k^2\rho_a^2(r_n/R+\delta/f)^2\right], \tag{12}$$

where r_n is the radius vector of the n-th point source.

It is obvious that the mean size of these images is approximately $\lambda f/\rho_a$, and if $S_0/R \lesssim 5\lambda^2/\rho_a^2$, then each spot occupies a substantial part of the area of the image. Let us estimate the dispersive power, or what is the same thing, the mean contrast in the distribution of intensity in this spot:

$$\sigma_I^2/\langle I_n\rangle^2=(\langle I_n^2\rangle-\langle I_n\rangle^2)/\langle I_n\rangle^2\approx 2\sigma^2\rho_a^2/S. \tag{13}$$

It is obvious that the dispersive power increases with an increase in σ and ρ_a and with $\sigma = 0.6$ and $\rho_a = 0.35\sigma_I/I = 2 \times 0.3 \times 0.5 = 0.3$ reaches a considerable value. The fact that the dimensions of spots are comparable with the size of the image and fluctuations in intensity in spots are great with relatively high σ and ρ_a results in considerable distortions of the image. In order to smooth out these distortions and at the same time to improve the image, it is necessary to accumulate a sufficiently great number of realizations of images for different realizations of amplitude distortions. In this case the distribution of intensity in the image is determined by equation (8) from which it is obvious that

on the condition that $1 << M \leq 5S/\rho_a^2$ the image on average is modeled by the smooth function $\exp[-(1/4)k^2\rho_a^2(r/R + \delta/f)^2]$, which makes it possible to determine the contours of the image.

The theoretical results arrived at above were confirmed experimentally. A diagram of the setup with which a study was made of the influence of amplitude distortions on the image of a diffuse object is shown in fig 1. The beam of an LG-38 helium-neon laser, 1, (λ = 632.8 nm), broadened by microlens 2 with a point diaphragm, 3, (diameter of approximately 20 μ) illuminated a model of a diffuse object, 4, executed in the form of a square opening measuring 3.5 X 3.5 mm in a nontransparent mask applied to a diffuse matte plate. The radiation scattered by the diffuse object fell onto a collecting lens, 5, with a focal length of f = 110 mm, which through diaphragm 6 with a diameter of 3 mm formed an image of the object. Amplitude mask 7 was made so that the optical density of the mask would be distributed according to a law close to normal for different parameters of σ and ρ_a. Microlens 8 formed a magnified image of object 4, which was recorded by a camera, 9, on RF-3 photographic film.

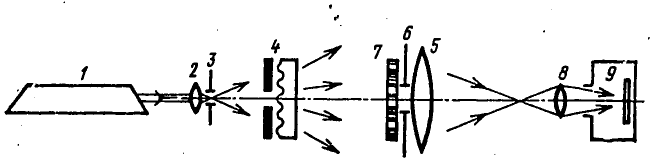

Figure 1. Diagram of Setup

The amplitude mask represented the distribution, recorded on "Mikrat-300" film, of intensity in laser radiation scattered for a matte diffuse glass. In fig 2 are given examples of negative images of amplitude masks used in this experiment with σ = 0.3 and $\rho_a \approx 1.1$ and 0.14 mm. The distance between object 4 and lens 5 was set equal to 567 or 1600 mm, i.e., so that with the selected object size and lens aperture the number of spots in the image of the object, M, would equal 400 or 500, respectively (cf. fig 3).

In fig 4 are shown images of the plane wave source--the point diaphragm, 3--obtained with the setup in fig 1 in the absence of object 4 without and in the presence of amplitude distortions.

It is obvious that in keeping with equation (11) with high σ and ρ_a the distribution in intensity in an image of this source (fig 4b) is distorted considerably, but the size of the image is not increased substantially. With high σ and low ρ_a (fig 4c), on the other hand, around a distinctly pronounced maximum is formed a broad background considerably weaker in intensity than the maximum. And, finally, with low σ (fig 4d) distortions are practically unnoticeable and the image is in the form of a typical "Airy spot" [4]. These data are explained well by equations (12) and (13).

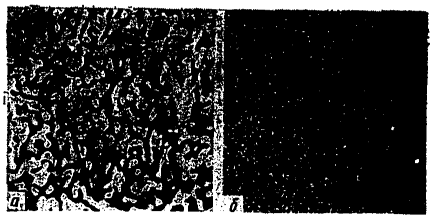

Figure 2. Negative Images of Amplitude Masks with $\sigma = 0.3$ and $\rho_a =$ = 1.1 (a) and 0.14 mm (b)

Figure 3. Images of Objects with a Number of Spots of $M = 400$ (a) and 50 (b)

In fig 5 are shown images of objects produced in the presence of amplitude distortions. The images of objects in fig 5a and 5c are characterized by a relatively low value of parameter $\eta = M\rho_a^2\sigma^2/S$ ($\eta < 0.1$); therefore distortions of the image are not too great. In fig 5b the typical size of one transformed spot in the image is considerably smaller than the size of the image itself, although η is high ($\eta > 0.15$); therefore it is outlined well and is practically not distorted (cf. equation (11)), since the condition $M >> S/\rho_a^2$ is fulfilled. Fig 5d illustrates the fact that with sufficiently high σ and M, but with low ρ_a, on the other hand, the background from each transformed spot exceeds the size of the image, and on the other hand, the total background from all these spots is comparable to the intensity of the majority of spots of the undistorted image, whereby

$\eta = M\rho_a^2\sigma^2/S \sim 0.1$. With a further increase in M (to $M \sim 2000$) distortions of the outline are practically not evidenced (similar to fig 5b).

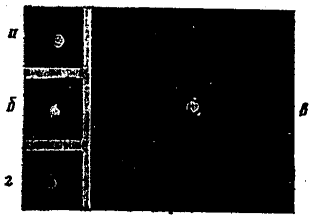

Figure 4. Image of Point Diaphragm in the Absence of Amplitude Distortions (a) and in the Presence of Distortions with $\sigma = 0.3$ (b,c) and 0.07 (d), and $\rho_a = 1.1$ (b,d) and 0.14 mm (c)

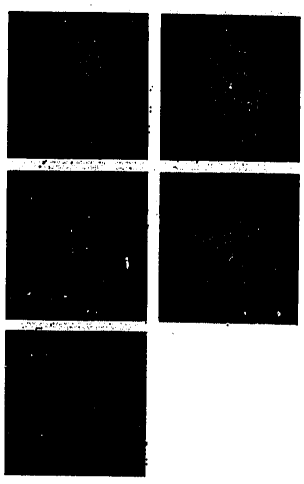

Figure 5. Images of Diffuse Objects in the Presence of Amplitude
[Caption continued on following page]

Distortions with $\sigma = 0.3$ (a,b,d,e) and 0.07 (c), and ρ_a = = 0.14 (a,d) and 1.1 mm (b,c,e) and $M = 50$ (a,c,e) and 400 (c,d)

In fig 5e the characteristic dimension of each transformed spot making up the image is comparable with the size of the image itself, and relative fluctuations in a spot are great, which results in distortion of the original contours of the image, although its total size practically does not change. In this case in accordance with equation (13) $\sigma_I/I \simeq 0.3$.

Finally, in fig 6 is shown the well outlined image of an object produced for $M = 50$, $\sigma = 0.3$ and $\rho_a = 1.1$ mm , corresponding to the case illustrated in fig 5e. It was produced with the accumulation of a sufficiently great number of realizations of images for different realizations of amplitude distortions by means of a sufficiently long exposure of the photographic film (approximately 1 s) with a moving amplitude mask, in total agreement with (8).

Figure 6. Outlining of Image of Object with $\sigma = 0.3$, $\rho_a = 1.1$ mm and $M = 50$ with the Accumulation of a Sufficient Number of Realizations of Amplitude Distortions

And so, a randomly inhomogeneous medium with amplitude fluctuations can under certain conditions substantially distort the image of a diffuse object, whereby the most considerable distortions arise with a sufficiently high variance in the logarithm of amplitude distortions of $\sigma \geq 0.2$ under two conditions: 1) $\eta = M_1\sigma^2\rho_a^2/S \gtrsim 0.3$ and $M_1 \sim S/\rho_a^2$; 2) the correlation radii of distortions become comparable with the dimensions of the receiving aperture, i.e., $S/\rho_a^2 \lesssim 10$, and here $M_2 \gtrsim 10S/\rho_a^2$ and $\sigma\rho_a/\sqrt{S} \gtrsim 0.1$.

In the latter case it is possible to improve image quality by the accumulation of images produced with different realizations of amplitude distortions.

If objects are sufficiently extended (M is very high), then the conclusions regarding the introduction of distortions by a randomly inhomogeneous

medium are carried over to local sections of the image containing in the absence of distortions M_1 or M_2 spots, respectively, for the first and second conditions.

Bibliography

1. Bakut, P.A., Ustinov, N.D., Troitskiy, I.N. and Sviridov, K.N. ZARUBEZHNAYA RADIOELEKTRONIKA, No 1, 3 (1977).

2. Ustinov, N.D., Bakut, P.A., Barinov, V.V., Devyatkov, L.A., Mandrosov, V.I. and Troitskiy, I.N. KVANTOVAYA ELEKTRONIKA, 5, 1257 (1978).

3. Ishimaru, A. APPL. OPTICS, 16, 3190 (1977).

4. Born, M. and Vol'f, E. "Osnovy optiki" [Fundamentals of Optics], Moscow, Mir, 1973, p 365.

CSO: 1862
8831

UDC 621.378.3

XeCl AND XeF LASERS WITH COMBINED PUMPING

Moscow KVANTOVAYA ELEKTRONIKA in Russian Vol 6 No 10, 1979 pp 2103-2108
manuscript received 23 Jan 79

[Article by Yu.I. Bychkov, A.I. Gorbatenko, I.N. Konovalov, V.F. Losev and V.F. Tarasenko, USSR Academy of Sciences Siberian Division Institute of High Current Electronics, Tomsk]

[Text] An investigation is made of XeF and XeCl lasers excited by a discharge stabilized by a short electron beam. It is demonstrated that in an XeF laser the formation of excimer molecules takes place both as a result of ion-ion combination and by the interaction of excited Ar and Xe atoms with molecules of the halogen carrier. The maximum efficiency of an XeCl laser is realized with excitation by an electron beam. With the application of an electric field, the contribution of the discharge to radiation is observed only in modes with the substantial multiplication of electrons.

Investigations were made in [1-6] of excimer lasers utilizing molecules of KrF* and XeF* with combined pumping, whereby the discharge is supported by an electron beam in the pulse length range of 0.3 to 1 μs. With this method of excitation a contribution to the emission is made both by the electron beam and the discharge. In [5] a study was made of the stability of the discharge and it was demonstrated that the reason responsible for its contraction is gradual ionization and an avalanche-type buildup of electron density. A discharge of long duration can be stable only with field strengths at which capture compensates the multiplication of electrons in the gas resulting from ionization. The discharge energy under these conditions is spent basically on the formation of excited atoms, and it is obvious that the use of the combined method of excitation is feasible only for those gas mixtures in which the energy of excited atoms is effectively spent on the formation of excimer molecules.

In [7,8] we demonstrated that in combined pumping with the employment of an electron beam of short duration (approximately 50 ns) high pumping power is realized by the discharge, high values of parameter E/p are reached in the plasma, and the discharge mode can exist both with the multiplication of electrons and without it. These properties of the

discharge indicate its promise for the purpose of producing powerful radiation pulses of short length.

In this report an analysis is made of the optimal conditions for excitation for XeF and XeCl lasers when employing combined short-duration pumping.

The experimental setup consisted of an electron accelerator and a laser cavity. The accelerator formed a ribbon-type electron beam with an energy of approximately 150 keV, a current density of approximately 20 A/cm^2 and a length of $t_p = 50$ ns , which was injected into the discharge gap of the laser cavity through a window measuring 2.6 X 20 cm, closed by a piece of iron foil 25 μ thick. Investigations were made with an interelectrode gap of 1 to 2 cm. The discharge was supplied by a 70 nF capacitor and the inductance of the discharge loop equaled 34 nH. The cavity was formed by an opaque mirror with an aluminum coating and by a plane-parallel quartz plate. Gases of the following purity were used: Ar--99.985 percent, Xe--99.96 percent, CCl_4--chemically pure, and NF_3--industrial.

Laser Utilizing an XeF* Molecule

In fig 1a are shown typical oscillograms of the discharge current, $I_r(t)$, the voltage in the plasma, $U_{pl}(t)$, and the electron beam current, $I_p(t)$. The voltage in the plasma was measured experimentally by means of a capacitive divider connected to the cavity's electrodes. The measured values agree well with the calculated, which were determined by the difference in voltages in the capacitor and inductance by the equation $U_{pl}(t) = U_C(t) - LdI_r(t)/dt$, where $U_C(t)$ is the voltage in the capacitor and $LdI_r(t)/dt$ is the voltage in the inductance. Because of the influence of the inductance at the initial stage of the discharge the voltage in the plasma is low, and then increases suddenly and can exceed the initial charging voltage of U_0 .

From the current and voltage oscillograms was plotted the dependence of the change in electron density over time, $n_e(t)$. Here the dependence of the velocity of electrons, $v(E/p)$, was taken from [9] for a mixture of 95 percent Ar and five percent Kr. Let us note that the maximum values of dependences $n_e(t)$ and $I_p(t)$ do not agree. This is related to the fact that at the maximum of $I_p(t)$ the electrons have the greatest energy, and the greatest ionization capacity belongs to electrons with lower energy.

The $n_e(t)$ curve (cf. fig 1a) shows that in a mixture of $Ar:Xe:NF_3 = 375:5:1$ (pressure of $p = 4$ atm , distance between electrodes equals $d = 1$ cm) with a discharge voltage of $U_0 = 15$ kV and a current density of $j = 28$ A/cm^2 , the multiplication of electrons in the discharge practically does not take place. By the termination of the electron beam pulse the electron density equals approximately 15 percent of the maximum value. Therefore under these conditions the energy of the discharge is spent chiefly on the excitation of atoms of Ar and Xe. With a higher charging voltage of $U_0 \geq 20$ kV is observed the multiplication of

electrons in the discharge as the result of gradual ionization, and as of the moment of termination of the electron beam pulse the electron density in the discharge remains high. Thus, in a discharge supported by an electron beam of short duration, depending on the voltage applied, a discharge is realized either without the multiplication of electrons or with multiplication.

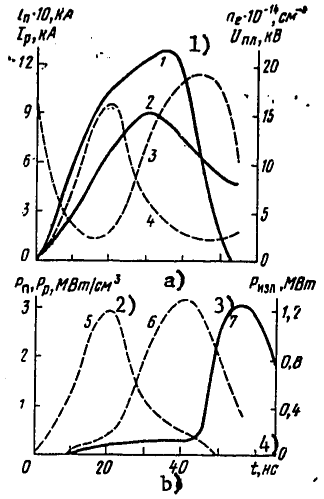

Figure 1. Dependences on Time of the Electron Beam Current (1), Discharge Current (2), Voltage in the Plasma (3) and Concentration of Electrons (4) and of the Power and Energy Contribution to the Gas, on the Beam (5), on the Discharge (6) and the Radiation Pulse (7)

Key:
1. U_{pl}, kV
2. MW/cm^3
3. P_{izl} [radiation], MW
4. t, ns

In fig 1b are shown dependences of the beam's power, $P_p(t)$, and discharge's power, $P_I(t)$, and radiation oscillograms obtained for conditions corresponding to fig 1a. The power contributed by the beam, $P_p(t)$, and the power of the discharge, $P_I(t)$, are shifted in time by 20 ns, which is responsible for the shape of the radiation pulse, which consists of two halves. The first, the initial, part of the radiation oscillogram depends only on the energy contributed to the gas by the beam, and the second on the energy of the discharge. This type of oscillogram makes it possible in principle to estimate the contribution to radiation of the beam and of the

discharge individually. For example, from the curves shown in fig 2 it can be concluded that with a voltage of U_0 = 15 kV the peak radiation power caused by the discharge is an order of magnitude greater than the radiation power from the beam.

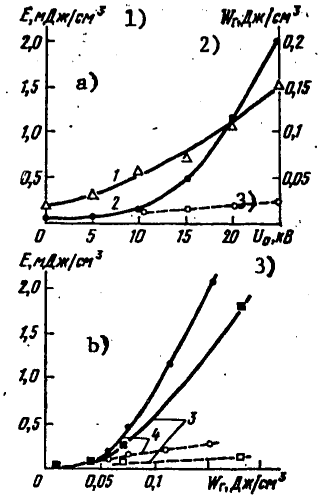

Figure 2. Dependence of the Energy Contributed to the Gas (1) and of the Radiation (2) on the Charging Voltage (a) and of the Specific Radiation Energy on the Energy Contributed to the Gas in Excitation by the Beam (3) and in Combined Pumping (4). Mixture of $Ar:Xe:NF_3$ = 375:5:1, p = 4 atm, d = 1 cm and j = 18 A/cm^2; the dotted line indicates radiation energy in the IR region of the spectrum.

Key:
1. E, MJ/cm^3
2. W_g, J/cm^3
3. U_0, kV

In fig 2a are shown dependences of the discharge energy, W_g, and radiation energy, E, on the charging voltage, U_0. With U_0 = 25 kV the discharge energy is approximately eightfold greater than the beam energy, and the radiation energy of approximately 1.6 mJ/cm^3 is produced practically on account of the discharge energy. Simultaneously with UV radiation was observed radiation in the near IR region of the spectrum, which can be related to familiar Xe* transitions [10]. With an increase in U_0 the energy of IR radiation increases insignificantly. The relationships

obtained demonstrate that in the excitation mode discussed is realized a high ratio of the discharge energy to the beam energy and the contribution to radiation is made chiefly by the discharge energy.

From an analysis of the curves shown in fig 1 it can be concluded that with $U_0 \leq 15$ kV the discharge energy is used basically to excite atoms. With the same voltage, according to the dependence of the radiation energy on U_0 (cf. fig 2a), the discharge energy makes a substantial contribution to the radiation. This makes it possible to assert that the formation of excimer molecules of XeF* takes place effectively without the formation of Xe^+ and Xe_2^+ ions.

For the purpose of comparing the effectiveness of the transformation of the beam energy and discharge energy into radiation, in fig 2 are shown dependences of the radiation energy on the energy put into the gas. Curves 3 were obtained in excitation with an electron beam alone. The energy put into the gas by the electron beam was determined by the procedure described in [7], taking into account the spectrum of electrons behind the foil and the scattering of electrons in the gas. Let us note that the energy put in by the beam, calculated by this procedure, proves to be approximately 1.5-fold less than the energy calculated from an oscillogram of the discharge current employing the dependence $v(E/p)$ from [9].

Curves 1 and 4 were obtained in excitation by a discharge supported by the beam, whereby the energy put into the gas by the beam did not exceed 0.02 J/cm^3. It is obvious from comparing these curves that the efficiency of a laser with excitation by a discharge supported by the beam is higher than with excitation by the electron beam alone.

Laser Utilizing an XeCl* Molecule

In the excitation of a mixture of Ar-Xe-CCl_4 by an electron beam utilizing a molecule of XeCl was produced radiation with an efficiency of approximately three percent and a specific radiation energy of $E_0 = 10$ J/l [7]. In connection with the high efficiency of an XeCl laser it was of interest to reveal the characteristics of this laser in excitation by a discharge supported by an electron beam. As for an XeF laser, a measurement was made of the energy introduced into the gas by the beam and discharge, and an estimate was also made of the efficiency of the conversion of each of these kinds of energy into radiation.

Oscillograms of the beam current, $I_p(t)$, discharge current, $I_r(t)$, voltage in the plasma, $U_{pl}(t)$, discharge power, $P_r(t)$, and radiation pulse with different charging voltages, U_0, are shown in fig 3. Since the content of CCl_4 in the mixture is low, then on the oscillogram for $I_r(t)$ is not observed a lowering of current associated with a lowering of the current of the electron beam. The semi-self-maintained discharge changes into a discharge with the multiplication of electrons. After the termination of the electron current pulse, depending on U_0 contraction

of the discharge can ensue. The voltage in the plasma is lowered with an increase in discharge current, and then increases, but unlike the discharge in working mixtures of the XeF laser does not exceed U_0. The discharge power maximum is reached as of the instant of termination of the electron beam pulse. Power maxima of the energy contribution to the gas by the beam and discharge are separated in time; therefore on the diation oscillograms are observed two components. Let us note that with low inductances of the discharge loop the power of the energy contribution from the discharge and electron beam, both for XeF and for XeCl lasers, coincide in time and the application of an electric field results in an increase in the amplitude of the radiation pulse. The change in the shape of the radiation pulse as a function of the voltage can be traced from the oscillograms in fig 3. An increase in radiation energy is observed only with relatively high voltages. In spite of the fact that the discharge energy put in is comparable to the energy put in from the beam, with a voltage in the gap of 10 kv the radiation pulse remains the same as with excitation by the beam alone.

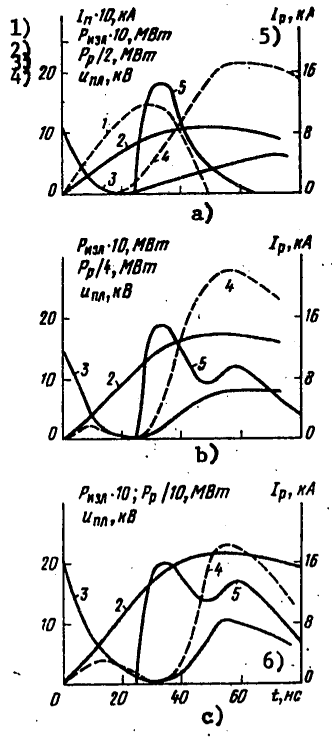

Figure 3. Dependence of the Electron Beam Current (1), Discharge
[Caption continuation and key on following page]

Current (2), Voltage in the Plasma (3), and Power Introduced into the Gas, on the Discharge (4), and of the Radiation Power (5) on Time. Mixture of $Ar:Xe:CCl_4$ = 2270:25:1, p = 3 atm, d = 2 cm, j = 28 A/cm^2; $U_0 = 10^4$(a), 15 (b) and 20 kV (c).

Key:
1. $I_p \cdot 10$, kA
2. $P^p_{iz} \cdot 10$, MW
3. $P_r/2$, MW
4. U_{pl}, kV
5. I^r, kA
6. t, ns

Dependences of the radiation energy, energy contribution and efficiency on the charging voltage are shown in fig 4. It can be concluded from these curves that the radiation energy with $U_0 \leq 10$ kV does not exceed the energy from the beam, and increases with higher U_0. The highest efficiency is realized in excitation by the beam ($U_0 = 0$) and equals approximately three percent. Maximum efficiency from the field, η = 2.5 percent, is reached with U_0 = 15 kV. With a maximum voltage of U_0 = 20 kV (a further increase in U_0 resulted in breakdown of the gap), the radiation energy increases threefold on account of the discharge, whereby the total efficiency of the laser equals approximately 2.5 percent. The share of radiation in the IR region of the spectrum did not exceed five percent of the radiation energy of an XeCl laser.

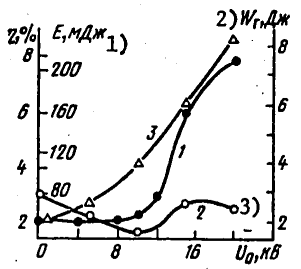

Figure 4. Dependence of Radiation Energy (1), Efficiency (2) and Energy Contributed to the Gas (3) on the Charging Voltage. Mixture of $Ar:Xe:CCl_4$ = 800:25:1, p = 3 atm, d = 2 cm, j = 20 A/cm^2, mean energy of electrons approximately 75 keV

Key:
1. E, mJ
2. W_g, J
3. U_0, kV

Thus, the dependences obtained demonstrate that the discharge energy makes a contribution to radiation in the case of high voltages at which the

effective multiplication of electrons takes place in the gas. The high efficiency of an XeCl laser with excitation by the beam as well as by the discharge in the mode including the multiplication of electrons proves that the formation of excimer molecules of XeCl* takes place more effectively with ion-ion combination. A discharge with the multiplication of electrons in the space for a short period (single numbers or dozens of nanoseconds) is contracted; therefore the excitation of an XeCl laser by a discharge supported by an electron beam of long duration is not efficient.

The radiation energy and efficiency of XeF and XeCl lasers achieved in this study are not the ultimate and can be increased by optimizing the cavity and excitation conditions.

Conclusion

The investigations made have demonstrated the following.

1. In an XeF laser with combined pumping the formation of excimer molecules takes place as the result of ion-ion recombination, and also in the interaction of excited atoms and molecules. Here with the excitation of an XeF laser by a discharge stabilized by a brief electron beam lasing efficiency is higher than in excitation by the electron beam.

2. An XeCl is one of the most efficient excimer lasers, and maximum efficiency is realized in excitation with the electron beam. With the application of an electric field a contribution of the discharge energy to the radiation takes place only in modes with the substantial multiplication of electrons. This demonstrates that the key role in the formation of XeCl* molecules is played by the ion-ion recombination of Xe and the halogen.

Bibliography

1. Mangano, J.A. and Jacob, J.H. APPL. PHYS. LETTS., 27, 495 (1975).

2. Bradford, R.S., Lacina, W.B., Avilov, E.R. and Bhaumik, M.L. OPTICS COMMS., 18, 210 (1976).

3. Mangano, J.A., Jacob, J.H. and Dodge, J.B. APPL. PHYS. LETTS., 29, 426 (1976).

4. Fisher, C.H. and Center, R.E. APPL. PHYS. LETTS., 31, 106 (1977).

5. Daugherty, J.D., Mangano, J.A. and Jacob, J.H. APPL. PHYS. LETTS., 28, 581 (1976).

6. Bychkov, Yu.I., Karlov, N.V., Konovalov, I.N., Mesyats, G.A., Prokhorov, A.M. and Tarasenko, V.F. PIS'MA V ZHTF, 3, 1041 (1977).

7. Bychkov, Yu.I., Konovalov, I.N., Losev, V.F., Mesyats, G.A., Ryzhov, V.V., Tarasenko, V.F., Fedorov, A.I., Shemyakina, S.B. and Yastremskiy, A.G. IZV. AN SSSR, SER. FIZICHESKAYA, 42, 2493 (1978).

8. Bychkov, Yu.I., Karlov, N.V., Losev, V.F., Mesyats, G.A., Prokhorov, A.M. and Tarasenko, V.F. PIS'MA V ZHTF, 4, 83 (1978).

9. Long, W.H. APPL. PHYS. LETTS., 31, 391 (1977).

10. Newman, L.A. and De Temple, T.A. APPL. PHYS. LETTS., 27, 678 (1976).

CSO: 1862
8831

UDC 621.3758

MEASUREMENT OF THE DISTRIBUTION OF THE INTENSITY OF LASER RADIATION BY MEANS OF BRAGG OPTICAL DIFFRACTION

Moscow KVANTOVAYA ELEKTRONIKA in Russian Vol 6 No 9, 1979 pp 2131-2138
manuscript received 27 Aug 78, after correction 2 Jan 79

[Article by V.V. Morozov, V.K. Petrov and Ye.F. Shershun, USSR Academy of Sciences Physics Institute imeni P.N. Lebedev, Moscow]

[Text] The necessary estimates are made and it is demonstrated experimentally that Bragg optical diffraction employing ultrasonic waves in air can be used for the purpose of measuring the distribution of the intensity of laser radiation. For the purpose of implementing this technique, an emitter is created, based on an X-cut of a quartz crystal. A measurement is made of the angular distribution of the ultrasonic field and a determination is made of its divergence, equal to $4 \cdot 10^{-3}$ rad at a frequency of 0.9 MHz. For the purpose of confirming the feasibility indicated here, a measurement is made of the distribution of laser radiation at a wavelength of 0.6328 μ in the fundamental and Bragg-diffracted radiation.

Introduction

As is known, the results of research on the optical diffraction of light by employing ultrasonic waves (Raman-Nato diffraction and Bragg optical diffraction) have resulted in important practical applications [1,2]. By means of optical diffraction it is possible to measure the speeds of sound and elastic constants in different media and to study the distribution of the intensity of an elastic wave inside a model. This phenomenon is of great importance in the creation of laser technology devices. Under this heading come different kinds of light modulators and deflectors and optical devices.

The intense development and introduction of different types of lasers have confronted investigators with new problems relating to measuring the radiation characteristics of these instruments. Under the heading of these problems must be placed increasing the accuracy of measuring divergence

and measuring the radiation distribution of lasers in the IR range [3]. It is of great interest to utilize the results of research on optical diffraction for these purposes, since optics introduced into powerful radiation can collapse. Below we make the necessary estimates and demonstrate that Bragg diffraction employing an ultrasonic wave in air can be used for the purpose of diverting a slight portion of the energy while preserving the space-time characteristics of the radiation.

For the practical realization of this technique are required high-Q ultrasonic wave emitters with a frequency of about 10^6 kHz and good directivity and spatial homogeneity of the ultrasonic radiation. We have made an ultrasonic cell based on an X-cut of a quartz crystal measuring 1 X 10 X 10 cm which satisfies these conditions, and a number of experiments have been performed which relate to the development of a procedure for measuring the distribution of laser radiation.

1. Optical Diffraction Employing Ultrasonic Waves

As is known [1], there exist two modes of optical diffraction: Raman-Nato and Bragg. Ordinary diffraction (Raman-Nato) employing ultrasonic waves takes place as the result of multiple scattering, if the angular distribution of the wave vectors of the elastic wave, q , is great as compared with the Bragg angle, θ_B , which is determined from the condition

$$K_p - K - q = 0$$

(K and K_r are the wave vectors of the incident and scattered light).

The boundary between the two modes is determined by the magnitude [2,4]

$$Q = 2\pi\lambda L/\Lambda^2, \tag{1}$$

where λ is the wavelength of the light; Λ is the wavelength of the sound; and L is the width of the acoustic beam.

The limiting case of $Q > 1$ defines the Bragg region of optical diffraction. At this limit the key requirement for the origin of effective diffraction is fulfillment of the Bragg condition. Here there arises only one order of diffracted light. On the other hand, $Q < 1$ defines a region of ordinary diffraction in which can be observed many orders of diffracted light.

Let us consider the region of Bragg diffraction. Condition $Q > 1$ must define one of the boundaries for the wavelength of sound with given L and λ :

$$\Lambda < |\sqrt{2\pi\lambda L}|. \tag{2}$$

On the other hand, the absorption of ultrasonic waves in propagation in a medium [1] is

$$\alpha=A\Omega^2 \tag{3}$$

(Ω is the frequency of sound and A = const); therefore it is necessary that with a given diameter of the light beam, d ,

$$\alpha d \leqslant 1. \tag{4}$$

Taking (2) to (4) into account, it is possible to write

$$|\sqrt{\lambda d}|v \leqslant \Lambda < |\sqrt{2\pi\lambda L}|, \tag{5}$$

where v is the velocity of sound in the medium.

The diffracted light maximum takes place at a Bragg angle of

$$\theta_B=\arcsin(q/2\varkappa)\approx\lambda/2\Lambda, \tag{6}$$

and the angle between the passing and scattered light beams equals

$$\theta_p=2\theta_B=\lambda/\Lambda. \tag{7}$$

If the divergence of the laser radiation, ϕ , is greater than the divergence of the acoustic beam, ψ , then the intensity of the diffracted light is reduced to half the maximum value at an angle of $\psi_{1/2}$, governed by the divergence of the acoustic beam [5]:

$$\psi=\Lambda/L, \qquad \psi_{1/2}=\Lambda/2L. \tag{8}$$

On the contrary, if $\psi > \phi$, then in the scattered light must be preserved the space-time characteristics of the incident radiation, i.e., $\phi_r \backsimeq \phi$.

The distance at which the deflected light beam leaves the primary radiation can be found from the equation

$$l \geqslant d[\theta_p - \varphi/2 - \min\{\varphi/2, \psi/2\}]^{-1}. \tag{9}$$

Now it is necessary to find the required value of the intensity of ultrasound for the purpose of arriving at real scattering coefficients and to determine the dynamic range (in relation to the intensity of the light and sound) of the technique under discussion.

The dynamic range in terms of the intensity of light in Bragg diffraction employing ultrasonic waves will be determined by the VRMB [expansion unknown]. In this case, in discussing the VRMB it is of interest to reveal how the intensity of the scattered light and ultrasonic wave will behave when the intensity of the scattered radiation is still much lower than the intensity of the exciting light ($I_r \ll I$) and, consequently, it is possible to assume that the strength of the exciting wave does not depend on the coordinates. By solving the Maxwell equations and equations for the motion of the medium, when the projections of the wave vectors of the scattered light and elastic wave onto the sense of the wave vector of the exciting light have the same direction (i.e., $0 < \theta_r < 90°$), it is possible to get [6]

$$|\mathbf{E}_p(x)|^2 = (g_{K_p}/g_q)\, P_0^2 \operatorname{sh}^2(\mathbf{E}\sqrt{g_{K_p} g_q}\, x),$$
$$|P(x)|^2 = P_0^2 \operatorname{ch}^2(\mathbf{E}\sqrt{g_{K_p} g_q}\, x) \tag{10}$$

with boundary conditions of $E_r(0) = 0$ and a pressure of $P(0) = P_0$. Here

$$g_{K_p} = \frac{(\rho \partial \varepsilon/\partial \rho)\,\beta_s\,|K_p|}{2\cos(K_p^{\wedge} x)}; \quad g_q = \frac{(\rho \partial \varepsilon/\partial \rho)\,|q|}{16\pi \cos(q^{\wedge} x)};$$
$$g_{K_p},\ g_q > 0;\ \beta_s = \frac{1}{\rho v^2};\ \left(\rho \frac{\partial \varepsilon}{\partial \rho}\right)^2 \approx 4(n-1)^2.$$

The condition for the lack of an influence of the exciting and scattered light waves on the nature of the medium's motion is

$$P_0 = P(0) \approx P(x) \approx \text{const}.$$

Taking this condition into account, from (10) we get

$$\operatorname{ch}(\mathbf{E}\sqrt{g_{K_p} g_q}\, x \approx 1);\ |(\mathbf{E}\sqrt{g_{K_p} g_q}\, x)^2| \ll 1. \tag{11}$$

From expression (11) it is possible to determine the limiting intensity of the exciting light with $x \gtrsim d\theta_B = d\lambda/(2\Lambda)$:

$$\frac{E^2}{4\pi} \ll \rho \left[\frac{v\Lambda}{\pi (n-1) d}\right]^2. \tag{12}$$

For pulsed radiation this value will be greater, since it is necessary to multiply it by $\tau/\Delta t_i$ [7,8], where τ is the time for the establishment of ultrasonic waves and Δt_i is the length of the pulse.

Then, from solving (10) for scattered light in fulfilling the conditions in (11), taking into account the fact that $P_0^2 \sim 2I_{zy}$ [sound] ρv, it is possible to arrive at the scattering coefficient for Bragg diffraction ($R_{max} \leq 0.01$):

$$R = \left|\frac{E_p}{E}\right|^2 = g_{K_p}^2 P_0^2 L^2 \approx \left[\frac{2\pi (n-1) L}{v\lambda}\right]^2 \frac{2I_{зв}}{\rho v}. \tag{13}$$

This relationship can be expressed in terms of Q, scattering angles and divergence of the acoustic beam, by employing (1), (7) and (8):

$$R = \frac{2(n-1)^2}{\rho v^3} \frac{I_{зв}}{\theta_p^4} Q^2 = \frac{8\pi^2 (n-1)^2}{\rho v^3 \theta_p^2} \left(\frac{I_{зв}}{\psi^2}\right). \tag{14}$$

It is obvious from (14) that the scattering coefficient is proportional to Q^2 and depends on the angular distribution of the intensity of the ultrasonic radiation. Relationship (13) is equivalent to the relative intensity at the maximum of the diffracted beam in an approximation of low amplitudes of the scattered light and ultrasonic waves [2].

At the present time there exists a somewhat arbitrary division of ultrasonic waves into waves of low and finite amplitude. In the process of propagation of a sound wave its shape can be distorted [9]. In this connection it is necessary for us to determine the range of variation of the sound's intensity so that over the entire spatial area of interaction between the light and sound equation (13) will be fulfilled, i.e., the scattering coefficient will depend linearly on the intensity of the sound. For this it is sufficient that the width of the light beam, d, be less than the distance which the sound wave travels to the point of formation of a break [9], i.e.,

$$d \leqslant \frac{\Lambda v}{\pi (\gamma_0 + 1) [2I_{зв}/(\rho v)]^{1/2}}. \tag{15}$$

For gases $(\gamma_0 + 1)/2 \sim 1.1$ to 1.3. Transforming equation (15), we get the maximum intensity of sound which can be used in the technique suggested:

$$I'_{\max \text{ зв}} = \frac{\rho v}{2}\left[\frac{\Lambda v}{\pi(\gamma_0+1)d}\right]^2. \tag{16}$$

Substituting the result obtained in equation (13), we have

$$R'_{\max} = \left[\frac{2}{\gamma_0+1}\,\frac{(n-1)}{\theta_p}\,\frac{L}{d}\right]^2. \tag{17}$$

The minimum coefficient is determined by thermal and aerosol scattering of the light [6]. Under actual conditions of conducting experiments they can be disregarded.

In the equations used above we did not take into account reflections of light from the boundaries of the medium in which the ultrasonic waves are propagated. In studies performed in recent times [10,11] it is demonstrated that the amplitudes and phases of the zeroth and first orders of a light wave passing through an ultrasonic beam in a homogeneous isotropic dielectric (in the case of angles close to the Bragg) depend on the reflection of light at the boundaries of the medium in which the sound is propagated. Therefore the technique under consideration can be implemented with minimum difficulties only for the case when ultrasonic radiation is propagated in air.

In the table are given the key parameters characterizing the Bragg optical diffraction of an ultrasonic wave in air ($\Omega = (0.3 \text{ to } 1)\cdot 10^6$ Hz) for an acoustic field depth of $L = 10$ cm and with $v \sim 3.3\cdot 10^4$ cm/s , $A \sim 10^{-13}$ s^2/cm , $n - 1 \sim 3\cdot 10^{-4}$, $\rho \sim 1.3\cdot 10^{-3}$ and $\phi \leq \psi$. As is obvious from this table, with certain parameters by means of Bragg diffraction it is possible successfully to divert a slight portion of the energy while preserving the space-time characteristics of the primary radiation in the diverted beam and thereby leaving the primary radiation practically undisturbed.

2. Ultrasonic Emitter

As has been demonstrated, the scattering coefficient in Bragg diffraction depends heavily on the angular distribution of the ultrasonic radiation (cf. (14)). On the other hand, for the purpose of increasing the accuracy of measurements it is necessary that the divergence of the scattered light on account of the finite nature of the frequency band of the ultrasonic emitter be negligibly slight. It is possible to disregard the increase in the divergence on account of the absorption of sound in air at frequencies of lower than 10^6 Hz, since $\Delta\Omega_n = \alpha v/\pi$, $\phi_{\Delta\Omega_n} = \lambda\alpha/\pi \sim 3\cdot 10^{-6}$ to $3\cdot 10^{-5}$, $\lambda = 10.6\ \mu$, and $\Omega = 3\cdot 10^5$ to $3\cdot 10^6$ Hz .

Table

1) d, см	2) λ, мкм	$\lvert\sqrt{A}d\rvert$, см	Λ, см	$\sqrt{2\pi\Lambda L}$, см	3) Ω, МГц	4) $\psi=\frac{\Lambda}{L}$, мрад	αd	$\left[\frac{R_{max}}{R_{min}}\right]^2$	5) $I_{пр}$, ГВт/см^2	Q	θ_p, мрад	* $I_{зв}$, МВт/см^2	l, м
5	0,6328 1,06 10,6	$0,72\cdot10^{-2}$	$3,3\cdot10^{-2}$	$6,3\cdot10^{-2}$ $8\cdot10^{-2}$ $26\cdot10^{-2}$	1	3,3	0,05	10^{-2}	10^{2}	4 6,6 66	1,8 3 30	2 5 50	2,5 1,7 0,17
10	10,6	$3,3\cdot10^{-2}$	$3,3\cdot10^{-2}$ 10^{-1}	$26\cdot10^{-2}$	1 0,33	3,3 10	1 0,1	10^{-4} 10^{-3}	0,1 1	66 6,6	30 10	0,5 5	3,3 10

* При $\varphi=\psi$ 7)

Key:

1. cm
2. μ
3. MHz
4. mrad
5. GW/cm^2
6. MW/cm^2
7. When $\phi = \psi$

The requirement of a high Q for the ultrasonic emitter, as well as of high homogeneity for the ultrasonic field imposes definite stipulations on the selection of an ultrasonic emitter for its use as a diverting unit in measuring the characteristics of laser radiation. This requirement can be satisfied by selecting an ultrasonic emitter based on an X-cut of a quartz crystal. For example, according to [2], for a quartz emitter vibrating in air the quality factor equals $G \simeq 5\cdot10^4$, and therefore for ultrasonic frequencies of $\Omega = 10^6$ Hz,

$$\varphi_{\Delta\Omega_G} = \frac{\lambda}{v}\,\Delta\Omega_G = \frac{\lambda\Omega}{vG} \ll 10^{-6}.$$

With thicknesswise vibrations of a quartz plate, different sections of its surface vibrate with different amplitudes and phases [2]. This irregularity in motion is caused by the quality of plates, as well as by the excitation in the plate of lengthwise oscillations as the result of transverse compression; therefore the lengthwise dimension of the plate should be much greater than its thickness. In this case the field of the ultrasonic plate can be regarded as the vibrations of a group of slightly directional emitters which because of the close distance between one another form a pencil beam emitter with a concentration factor with regard to the main direction of [12] $\gamma \simeq 4\pi S/\Lambda^2$, where S is the area of the plate. The

The directivity for a group of contiguous emitters or the divergence of the ultrasonic beam in the far-range field (the case of high frequencies, $qr >> 1$) is given by the expression $\psi = \Lambda/L$. Thus, with this consideration an ultrasonic quartz emitter should create a homogeneous acoustic field.

On the basis of the above, we designed an emitter based on an X-cut of a quartz crystal measuring 1 X 10 X 10 cm, shown in fig 1 [photograph not reproduced]. The natural frequency of the fundamental vibration of such an emitter, thicknesswise, equals [2] $\Omega_0 \simeq 2280/d_k \simeq 0.3 \cdot 10^6$ Hz . Since in quartz it is possible easily to excite a sufficiently great number of odd-parity orders, then such an emitter can be discretely frequency tuned by varying the frequency of the electrical voltage applied.

3. Experimental Investigation of the Field of an Ultrasonic Emitter by Means of Bragg Diffraction

A diagram of the experimental setup is shown in fig 2. As the source of light radiation was used a single-mode He-Ne laser of the LG-38A type ($\lambda = 0.6328$ μ) with a divergence of $\phi = 3 \cdot 10^{-4}$ and $d = 0.3$ cm . The laser's radiation, passing through the diaphragm and a mechanically modulated modulator ($f = 10^3$ Hz), intersected the ultrasonic field ($\Lambda = 4 \cdot 10^{-2}$ cm) created by the quartz cell, at the Bragg angle. The diffraction pattern was studied by the photoelectric method. In fig 3 is shown the diffraction pattern of the light radiation passing through the ultrasonic field. It is obvious that the divergence of the laser radiation in diffraction orders agrees with the divergence of the laser radiation striking the ultrasonic field; the scattering factor for the $\pm$ 1-th order is $R \simeq 10^{-3}$.

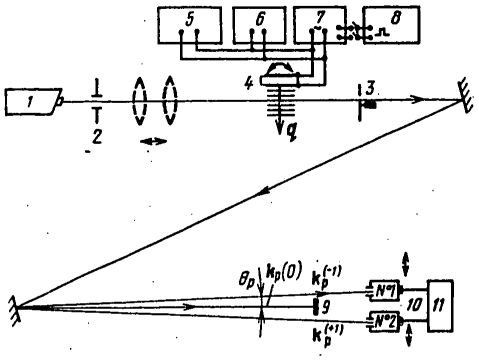

Figure 2. Diagram of Experimental Setup: 1--LG-38A laser; 2--diaphragm; 3--chopper; 4--quartz cell; 5--freq-meter; 6--

[Caption continued on following page]

voltmeter; 7--ultrasonic oscillator; 8--modulator; 9--screen; 10--FEU-62 [photomultiplier]; 11--S1-17 oscillograph

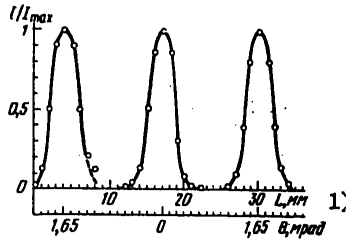

Figure 3. Distribution of Laser Radiation, Incident and Diffracted by $\pm$ 1 Order, with a Quartz Emitter Frequency of 871 and 667 kHz

Key:
1. mrad

The diffraction maxima are shifted relative to the radiation direction, K , by an angle agreeing with the scattering angle in (7):

$$\theta_p=\lambda/\Lambda=1{,}66\cdot10^{-3}.$$

The distribution of vectors, q , of the ultrasonic field can be registered in swinging the ultrasonic cell about the Bragg angle, if thereby the angle between the incident light beam and the detected beam is kept constant, since $\phi < \psi$. As is obvious from fig 4, the angular distribution of ultrasound at the major maxima is sufficiently homogeneous, without any "spikes" or "dips." The divergence of the ultrasonic field, determined in relation to half of the range of the maximum value in the distribution, is close to the diffraction and equals $\psi \simeq 4.0\cdot10^{-3}$ rad . The secondary maxima in fig 4 originate as the result of diffraction in the oblique incidence of a laser beam onto an ultrasonic field of finite width [1].

For the purpose of verifying the homogeneity of the ultrasonic field in terms of the wave vector, q , we also plotted the dependence of the amplitude of the diffracted light on the distance from the place at which the light intersects the ultrasonic wave to the plane of the quartz emitter (fig 5). Since the ultrasonic field has sufficiently not too great a divergence ($\psi \simeq 4.0\cdot10^{-3}$), then at distances of up to 10 cm the intensity of sound waves should be governed by the absorption of sound in the air. On the other hand, the intensity of the diffracted light equals

$$I \sim I_{зв} = I_0 e^{-2\alpha x},$$

Therefore the slope of the straight line (cf. fig 5) should determine the absorption of sound, $\alpha = 0.25\ cm^{-1}$. Absorption determined in this manner agreed with that measured previously in [1].

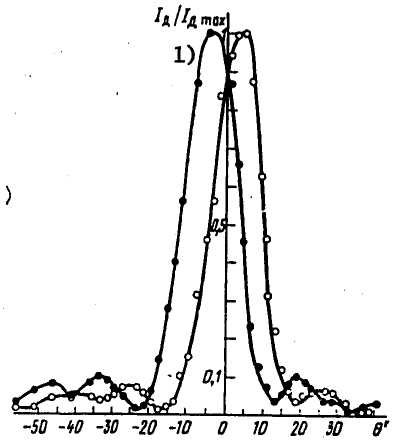

Figure 4. Intensity of Radiation Diffracted by ± 1 Order as a Function of the Angle of Incidence of the Light Onto the Ultrasonic Wave

Key:
1. $I_d/I_{d\ max}$

The experiments conducted have demonstrated that the selected type and geometry of the ultrasonic emitter, as well as the modern technology for its fabrication, make it possible to create an ultrasonic field homogeneous in space, by means of which it is possible in the Bragg optical diffraction mode to make precise measurements of the space-time characteristics of laser radiation. If the diameter of the laser radiation is comparable to the diameter of the ultrasonic emitter's plate, then it is necessary to take into account modulation of the ultrasonic field on account of bending vibrations [14].

By means of Bragg optical diffraction utilizing ultrasonic waves created by emitters of this type it is possible to measure the divergence of optical radiation [5,13].

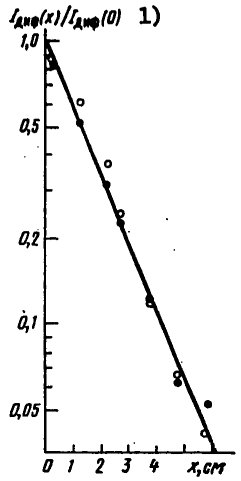

Figure 5. Dependence of the Amplitude of Light Diffracted by +1 (White Dots) and -1 (Black Dots) Order on the Distance From the Place at Which the Light Intersects the Ultrasonic Wave to the Plane of the Quartz Emitter

Key:

1. $I_{dif}(x)/I_{dif}(0)$

Bibliography

1. Bergman, L. "Ul'trazvuk" [Ultrasound], Moscow, IL, 1957.

2. Mezon, U. and Tereton, R. "Fizicheskaya akustika, printsipy i metody" [Physical Acoustics, Principles and Methods], Vol VII, Moscow, Mir, 1974.

3. Nickel, G.H., Goodfellow, G.M. and Terwilliger, D.F. IEEE J, QE-5, 20 (1972).

4. Rytov, S.M. IZV. AN SSSR, SER. FIZICHESKAYA, 2, 223 (1937).

5. Gordon, E.I. APPL. OPTICS, 5, 1629 (1966).

6. Fabelinskiy, I.L. "Molekulyarnoye rasseyaniye sveta" [Molecular Scattering of Light], Moscow, Nauka, 1965.

7. Starukov, V.S. and Fabelinskiy, I.L. UFN, 98, 441 (1969).

8. Gorbunov, L.M. ZHETF, 65, 1337 (1973).

9. Zarembo, L.K. and Krasil'nikov, V.A. UFN, 18, 687 (1959).

10. Ctyroky, I. OPTICS COMMS., 16, 259 (1976).

11. Zil'berman, G.Ye. and Kupchenko, L.F. RADIOTEKHNIKA I ELEKTRONIKA, 22, 1551 (1977).

12. Tyulin, V.N. "Vvedeniye v teoriyu izlucheniya i rasseyaniya zvuka" [Introduction to the Theory of the Transmission and Scattering of Sound], Moscow, Nauka, 1976.

13. Walder, J. and Tang, C.L. PHYS. REV., 19, 623 (1967).

14. Osterberg, H. J. OPT. SOC. AMER., 23, 30 (1933).

CSO: 1862
8831

UDC 621.373.862

EQUILIBRIUM CHEMICAL COMPOSITION OF GASES IN A SEALED HIGH-PRESSURE CO_2 PULSED LASER

Moscow KVANTOVAYA ELEKTRONIKA in Russian Vol 6 No 10, 1979 pp 2160-2165
manuscript received 14 Dec 78, after correction 19 Mar 79

[Article by V.S. Aleynikov, V.K. Sysoyev and Yu.F. Bondarenko]

[Text] An investigation is made of the dynamics of the change in and establishment of the equilibrium chemical composition of the gas mixture in a pulsed high-pressure CO_2 gas discharge laser with preliminary photoionization and a high current pulse repetition rate with transverse pumping of the gas in a closed cycle. The employment of a high current pulse repetition rate is conducive to rapid establishment of an equilibrium chemical composition of the mixture (in 10 to 15 min) in a relatively large volume (60 liters) without substantial contamination of the mixture with desorbed gases. It is established that upon expiration of this time interval, after the discharge is started, in the gas volume is established dynamic equilibrium between the reactions for the dissociation of CO_2 molecules and the recombination of dissociation products. It is demonstrated that the steady-state degree of dissociation of the carbon dioxide is a function of the electrical parameters of the discharge and the original composition of the gas mixture and does not depend on the pressure. Under typical conditions of a laser discharge, the steady-state degree of dissociation of CO_2 molecules equals 20 to 30 percent. A demonstration is given of the feasibility of using hydrogen as a catalyst for the reaction of the oxidation of carbon monoxide. Based on investigations conducted, it is recommended that lower mixture pressures be used for operating modes of practical importance, of pulsed CO_2 lasers utilizing chemical-equilibrium mixtures.

1. A key problem in the development of pulsed high-pressure CO_2 lasers with a transverse discharge (TEA lasers) is the realization of a homogeneous space discharge [1]. One of the factors influencing the stability of the discharge is the presence in the gas mixture of oxygen, which appears in the plasma of the pulsed discharge as a result of the dissociation of CO_2 molecules [2]. The presence of oxygen in an amount of a few percent at atmospheric pressure of the gas mixture in a pulsed transverse

discharge with preliminary photoionization is conducive to the development of spatially localized arcs [3]. Since the appearance of arcs results in inhomogeneous excitation of the space with the laser mixture, the energy characteristics of the laser depend to a strong extent on the rate of chemical reactions activated by the plasma's electrons. Therefore an important objective is an investigation of the change in the composition of the gas mixture during the time the discharge is ignited and of the factors influencing the equilibrium composition of the mixture. This information is especially necessary for the development of sealed pulsed instruments and CO_2 lasers with a high pulse repetition rate. In the latter the high rates of dissociation of CO_2 molecules do not make it possible effectively to regulate the content of dissociation products without removing a considerable portion of the spent mixture. The need for this removal substantially complicates and makes more expensive the construction of TEA lasers.

2. An experimental investigation was made of the composition of the mixture in a setup whose key component consisted of a pulsed CO_2 laser with transverse excitation. A homogeneous pulsed discharge with high pressure of the gas mixture was initiated by means of UV preionization in a space of 1.3 X 2.6 X 35 cm. The current pulse repetition rate was 100 Hz. Transverse pumping of the gas mixture through a closed circuit made possible a gas rate in the discharge gap of about 20 m/s. Solid-profile electrodes made of copper and Duralumin were used. Investigations were made of the composition of the gas mixture for the percentage content of CO_2, O_2, CO and N_2 by the chromatographic method under conditions of a homogeneous space discharge.

The gas mixture was sampled in special glass containers whose volume equaled less than 10^{-4} the volume of the laser cavity, after fixed periods of the discharge's burning. For analysis was used an LKhM-8MD chromatograph with two columns, one with MSM silica gel at a temperature of 100°C, and the other with a 0.5 nm molecular sieve at room temperature. The carrier gas was helium, and the concentrations of components were determined by a heat conduction detector. The maximum sensitivity of the chromatograph for CO_2, O_2 and N_2 was 0.1 percent, and for CO, two percent; the error in determination of the relative concentration of gases was not greater than 10 percent.

3. In fig 1 are shown typical curves for the variation in composition of the gas mixture during the period the discharge is burning. As is obvious from fig 1, in the process of the discharge's burning there takes place the dissociation of CO_2 molecules and the formation of dissociation products CO and O_2. With the passage of time the rate of accumulation of dissociation products is slow, which indicates an increase in the rate of the reaction for the recombination of dissociation products. The chemical process which takes place can be described by the reversible reaction

$$CO_2 \rightleftarrows CO + {}^1/_2 O_2. \quad (1)$$

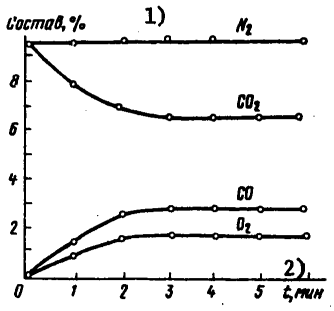

Figure 1. Change in Composition of a CO_2:N_2:He = 1:1:3 Gas Mixture with p = 1 atm in the Process of Discharge Burning. E/p = 21 V/(mm Hg·cm); C_S = 0.5 nF/cm^2 ; f = 100 Hz

Key:
1. Composition, percent
2. t , min

Between the forward and reverse reactions is established dynamic equilibrium, which governs the steady-state rate of dissociation of CO_2 and the content of dissociation products. In the state of dynamic equilibrium the rate of dissociation of CO_2 molecules, V_q , and of recombination of CO and O_2 molecules, V_r , are equal:

$$V_q = V_p. \tag{2}$$

The rate of dissociation of CO_2 molecules, according to the results of [2], equals

$$V_q = \frac{\alpha}{p} \frac{1}{e} C_S d_{AK} \frac{E}{p} p^2 f, \tag{3}$$

where α/p is the normalized dissociation coefficient, e is the charge of an electron, d_{AK} is the distance between electrodes, C_S is the storage capacitance normalized for the area of the electrode, E is the strength of the electric field, p is the pressure of the gas mixture, and f is the pulse repetition rate. Dependences of α/p on E/p and the composition of a CO_2-N_2-He mixture are given in [2].

It can be assumed that the reaction for the recombination of CO and O_2 molecules is a volume and bimolecular reaction and that the recombination

reaction rate does not depend on the pressure of the gas mixture [4]. Then the recombination rate equals

$$V_p = K_p n_{O_2} n_{CO}, \tag{4}$$

where n_{CO} and n_{O_2} are the concentration of molecules of CO_2 and O_2 and K_r is the recombination coefficient. Taking into account the fact that

$$n_{O_2} = {}^1/_2 n_{CO}, \quad n_{O_2} = \mathscr{L} p_{O_2}; \quad p_{O_2} = {}^1/_2 X_q p_{CO_2}, \quad p_{CO_2} = mp, \tag{5}$$

we get

$$V_p = {}^1/_2 K_p f X_q^2 m^2 \mathscr{L}^2 p^2, \tag{6}$$

where $L = 3.6 \cdot 10^{16}$ (mm Hg·cm^3)$^{-1}$ is the numerical factor for conversion from the measurement of V_r in cm^3/s to V_r in (mm Hg·s)$^{-1}$; X_q is the degree of dissociation of CO_2 molecules and m is the relative content of CO_2 in the gas mixture.

Utilizing equations (3) and (5), we find that the degree of dissociation, X_q^0, in the state of dynamic equilibrium equals

$$X_д^0 = \frac{1}{\mathscr{L} m} \left(\frac{2}{e}\right)^{1/2} \left(\frac{\alpha}{p} \frac{E}{p} C_S d_{AK} \frac{1}{K_p}\right)^{1/2}. \tag{7}$$

Measurement results arrived at with a constant value of E/p (fig 2) indicate the lack of dependence of the steady-state degree of dissociation on the pressure of the gas mixture. Since the activation of CO and O_2 in the gas discharge is carried out by electrons, then it is possible to assume that the magnitude of X_q^0 will depend on the composition of the gas mixture and the field strength normalized for the pressure.

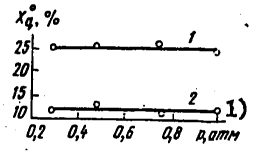

Figure 2. Dependence of Steady-State Degree of Dissociation of CO_2 on Pressure of the $CO:N_2:He$ = 1:1:8 (1) and 1:1:4 (2) Gas Mixture. E/p = 25 V/(mm Hg·cm) ; C_S = 0.5 nF/cm^2

[Key on following page]

Key:
1. p , atm

With the assumption made above regarding the volumetric nature of the recombination process, the degree of dissociation should not depend on the material of the electrodes. For the purpose of verifying this assumption, measurements were made of the steady-state values of concentrations of components of the mixture in a discharge with copper and Duralumin electrodes. The measurement results presented in the table demonstrate that within the limits of measurement error the degree of dissociation does not depend on the material of the electrodes.

Table. Values of Steady-State Degree of Dissociation of CO_2 for Different Combinations of Electrode Materials

Material of electrodes		X_q^0 , %
Cathode	Anode	
Cu	Cu	23
D16T	D16T	24
Cu	D16T	22.5
D16T	Cu	23.5

As we know [3], a content of oxygen in the gas mixture of a pulsed CO_2 laser equaling approximately 0.5 to 1.0 percent at atmospheric pressure of the working mixture results in arcing. Therefore it is important to disclose how the steady-state degree of dissociation of CO_2, determining the quantity of oxygen in the mixture, depends on the parameters of the electric circuit and the composition of the gas mixture. One of the key parameters characterizing the discharge circuit is the storage capacitance, C_S , reduced for the area of the cathode.

The steady-state degree of dissociation increases in proportion to $C_S^{1/2}$ and in the practically realizable range of $C_S \simeq 0.1$ to 0.5 nF/cm^2 reaches values of 13 to 30 percent, respectively. This dependence of the degree of dissociation on the reduced capacitance of the discharge substantially limits the unit energy contribution for sealed TEA CO_2 lasers with UV preionization.

The dependence of the degree of dissociation on the pulse repetition rate, described by the equation in [7], predicts a slow growth in the degree of dissociation with an increase in the repetition rate. A corresponding increase in the content of oxygen in the mixture with an increase in the repetition rate in the steady-state mode can limit the maximum realizable pulse repetition rate at which the homogeneity of the discharge is still maintained.

Taking into account the fact that CO_2 and N_2 are contained in the composition of an optimal laser mixture in a ratio of 1:1, and that the content

of helium, as a rule, can vary over a wide range, it is advisable to disclose the dependence of the steady-state degree of dissociation on the concentration of helium in a CO_2-N_2-He mixture. In fig 3 is shown the dependence of the steady-state degree of dissociation on the number of parts of helium at atmospheric pressure of the mixture (1). An increase in the degree of dissociation of CO_2 molecules with an increase in the helium content results in the fact that for gas mixtures with a different He content the percentage content of oxygen remains constant (curve 2 in fig 3).

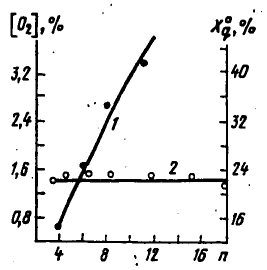

Figure 3. Dependence of Steady-State Degree of Dissociation of CO_2 (1) and of Oxygen Content (2) on the Number of Parts of Helium in a CO_2:N_2:He = 1:1:n Mixture. E/p = 24 V/ /(mm Hg·cm) ; $p \doteq 1$ atm , C_S = 0.5 (1) and 0.4 nF/cm^3 (2)

4. For the purpose of verifying the possibility of reducing the steady-state degree of dissociation of CO_2 by means of volumetric catalysis of the reaction for the oxidation of CO, measurements were made of the degree of dissociation of CO_2 in mixtures containing as a homogeneous catalyst an addition of hydrogen. The results of these measurements are shown in fig 4. The dependence obtained, of the degree of dissociation of CO_2 molecules on additions of hydrogen, can be explained in the following manner. With low quantities of hydrogen in the mixture, catalysis of the CO oxidation reaction results in a reduction in the degree of dissociation and in the concentration of its products, CO and O_2. With a hydrogen content greater than 10 percent, in addition to the CO oxidation reaction there evidently occurs the recombination of hydrogen with free oxygen formed in the dissociation of CO_2 molecules. When the hydrogen content is greater than 20 percent, the pressure of the CO again increases to the prior level and the degree of dissociation of CO_2 molecules increases. Here the pressure of the oxygen drops monotonically with an increase in the addition of hydrogen. The increase in the degree of dissociation of CO_2 molecules with a high content of hydrogen in the mixture is associated with the formation of water. Since the oxygen formed as the result of the

dissociation of CO_2 molecules is bound by the hydrogen, then reaction (1) shifts to the right as the result of an insufficiency of oxygen. Then in the mixture occurs a diminution of CO_2 molecules and a growth in the number of CO and H_2O molecules. Molecules of water are electronegative, and an increase in the stability of the homogeneous discharge with additions of hydrogen of greater than 10 percent is not expected. Thus, it can be concluded from fig 4 that the utilization of hydrogen as a catalyst for the oxidation of CO molecules in pulsed CO_2 lasers with a transverse discharge is limited to amounts of H_2 not exceeding 10 percent of the total pressure of the mixture.

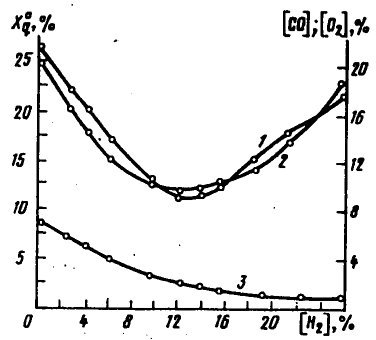

Figure 4. Dependence of Steady-State Degree of Dissociation of CO_2 (1) and of Content of CO (2) and O_2 (3) on Additions of Hydrogen. E/p = 25 V/(mm Hg·cm), p = 0.35 atm, C_S = = 0.3 nF/cm^2

5. It is known that additions of products of electrochemical interaction in the gas mixture result in the origin of instability of the discharge [3]. Presenting the greatest danger in this respect is oxygen. At atmospheric pressure additions of oxygen to the mixture in a quantity of 0.5 to one percent result in the appearance of arcs and in a severe worsening of the laser's energy characteristics. Since the steady-state degree of dissociation of CO_2 molecules, as demonstrated in this paper, is about 25 percent, it is obvious that at atmospheric pressure of the gas mixture the partial content of CO_2 molecules in the working mixture of a pulsed laser with a transverse discharge should not exceed three to four percent, if special measures are not taken for the purpose of speeding the recombination of oxygen with carbon monoxide. For the purpose of achieving reproducible energy characteristics for lasers at atmospheric pressure, the content of CO_2 molecules in the mixture should be even lower (on the order of one percent). However, with such a low content of CO_2 molecules in the working mixture, the energy of a pulsed laser is reduced 20- to 50-fold as

compared with the maximum achievable unit laser energy at atmospheric pressure (40 to 60 J/liter).

It is possible to achieve in two ways stable energy characteristics while preserving high unit energy in lasers employing a chemically equilibrium mixture. The first presupposes the employment of homogeneous and heterogeneous catalysis for the purpose of speeding the reaction for the recombination of the products of the dissociation of CO_2 molecules at high (equal to or greater than 1 atm) working pressures of the laser mixture. At the present time a sealed pulsed laser is known with atmospheric pressure of the mixture, in which the employment of both types of catalysis has made it possible to achieve a unit energy of 15 J/liter with an energy in the pulse of 0.5 J [3].

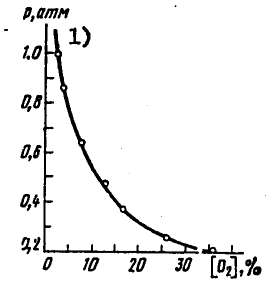

Figure 5. Dependence of Maximum Working Pressure on Additions of Oxygen to a CO_2:N_2:He = 1:1:3 Mixture. E/p = 25 V/ /(mm Hg·cm) , C_S = 0.5 nF/cm^2

Key:
1. p , atm

The second way consists in utilizing the dependence, found in this study, of the maximum operating pressure on additions of oxygen. The experimental dependence found is shown in fig 5. This curve was obtained in the following manner. At a certain operating pressure, to a laser mixture operating in the single pulse mode was added a gradually increasing addition of oxygen until the appearance of visually observable arcs and a sudden drop in output power. Thus was found the maximum permissible content of an addition of oxygen at a given pressure of the gas mixture. Then the working pressure of the mixture was changed and the measuring procedure was repeated. It can be concluded from the curve shown in fig 5 that the percentage of oxygen with a reduced pressure of the laser mixture can be

considerably higher than at atmospheric pressure. It is not difficult to see that with reduced pressure of the mixture utilization of the laser cavity in the sealed mode for chemically equilibrium mixtures will be more effective. Actually, for a mixture of CO_2:N_2:He = 1:1:3, producing a unit laser output of 25 J/liter·atm, the equilibrium pressure of hydrogen will equal about 2.5 percent. At atmospheric pressure, as already noted above and as can be concluded from fig 5, a stable discharge in a chemically equilibrium laser mixture in the absence of CO oxidation catalysts is practically impossible. At the same time, with a pressure of 0.5 atm, the unit output equals about 12 J/liter and a stable discharge is possible without using a catalyst.

Let us note that similar unit energies can be produced for chemically equilibrium mixtures also by employing catalyzation regulation of the reverse reaction for the recombination of CO and O_2 molecules [3]. However, the utilization of reduced pressures of the laser mixture has the advantage that in this case the discharge in chemically equilibrium mixtures lies far from the limits of instability for oxygen. Therefore a stable discharge and invariability of the energy characteristics of the laser can be expected for an extended period (of course, if other factors are eliminated which result in instability of the discharge, such as impurities in the form of other electronegative gases, field inhomogeneities, etc.).

6. As a result of the study conducted, it has been established that with the parameters of the electrical circuit and the composition of the CO_2-N_2-He gas mixture employed in TEA lasers utilizing carbon dioxide, as the result of the effect of the discharge on the gas is established a chemically equilibrium mixture of the gases CO_2-CO-O_2-N_2-He. The amount of oxygen formed at atmospheric pressure of a chemically equilibrium laser mixture lies, as a rule, in a range sufficient for contraction of a homogeneous space discharge.

The steady-state degree of dissociation of CO_2 for a specified initial mixture composition and field strength normalized for the pressure does not depend on the total pressure of the gas mixture and material of the electrodes; it increases with an increase in the content of helium in the mixture and in the magnitude of the unit storage capacitance. Slight additions of oxygen (up to 10 percent) result in a reduction in the steady-state degree of dissociation of CO_2.

The realization of pulsed lasers with a transverse discharge utilizing carbon dioxide having sufficiently high unit energy (25 J/liter·atm) and stable energy characteristics is facilitated by dropping the pressure of the working mixture below 1 atm. For the purpose of designing pulsed lasers of this sort, operating with chemically equilibrium mixtures (sealed mode or a mode with a high repetition rate without total renewal of the mixture), it is feasible to use working mixtures with a pressure on the order of 0.5 to 0.7 atm.

Bibliography

1. Vud, O.,II. TIEER, No 2, 83 (1974).

2. Smith, A.L. and Austin, Y.M. J. PHYS. D., 7, 314 (1974).

3. Stark, D., Cross, P.H. and Foster, H.A. IEEE J., QE-11, 774 (1975).

4. Avramenko, P.I. and Kolesnikov, R.V. IZV. AN SSSR, OTD. KHIMICHESKIKH NAUK, No 9, 1562 (1959).

CSO: 1862
8831

UDC 621.378.33

FEASIBILITY OF IMPROVING THE EFFICIENCY OF SEALED CARBON MONOXIDE LASERS

Moscow KVANTOVAYA ELEKTRONIKA in Russian Vol 6 No 9, 1979 pp 2195-2198
manuscript received 26 Mar 79

[Article by V.I. Masychev]

[Text] The results are given of an investigation of the possibility of improving the efficiency of sealed water-cooled CO lasers by reducing the total losses of the optical cavity. The experimentally realized efficiency of a laser emitter equaled 18 to 20 percent with a lasing power of about 32 W. A study is made of the influence of the temperature of the walls of the gas discharge tube on the efficiency and unit-length lasing power. In changing the temperature of the cooling fluid from 40 to 1°C the efficiency of the laser emitter increased from 8.5 to 18 percent, and the unit-length power from 13 to 31 W/m. The maximum lasing power equaled 38.5 W. Discussed briefly is the feasibility of further improving the efficiency of sealed CO lasers.

At the current time the experimentally realized efficiency of sealed CO lasers excited by an electric discharge and cooled by water at room temperature does not exceed eight to 12 percent [1,2] and is considerably inferior to lasers utilizing CO with other methods of excitation and systems for cooling the working gas mixture, which have an efficiency of greater than 40 percent [3]. At the same time, the undisputed design advantages (dispensing with cryogenic technology, pumping of the gas mixture, etc.) and the long service life in the sealed mode [2] have stimulated searches for ways of improving the lasing power and efficiency of this class of lasers.

The purpose of this study has been an experimental investigation of the feasibility of improving the efficiency of sealed water-cooled CO lasers.

1. As is known, the energy characteristics of lasers with relatively not too high gain can be improved considerably by reducing the total losses of the optical cavity. Preliminary estimates have indicated that as the result of reducing these losses the lasing power and efficiency of sealed water-cooled CO lasers can be increased at least twofold. On the basis of these estimates experiments were devised to verify the results obtained.

In the experiments were used gas discharge tubes made of molybdenum glass with a discharge section length of 125 cm and an inside diameter of 15 mm. The discharge was cooled by circulating water which usually had a temperature of 12 to 14°C. The tube was filled with a gas mixture of $Xe:CO:N_2:$:He = 2.1:1:3.4:16.5 with a total pressure of about 24 mm Hg.

Cavities with two inside mirrors were used. A totally reflecting gold mirror sprayed onto a Superinvar backing had a radius of curvature of 5 m. The outlet dielectric mirror on a potassium chloride backing was flat. The mirrors used in the experiments had a high quality finish on their reflecting surfaces. The totally reflecting mirrors were first tested by the moiré method. From a large lot of mirrors were selected mirrors with a regular moiré structure. The dielectric mirrors were tested for flatness interferometrically, using a mercury green line wavelength of $\lambda = 0.54\ \mu$, and had not more than three to five interference rings on a 35 mm diameter.

The reduction of total losses of the optical cavity resulting from dispensing with a Brewster window, which usually had losses of about two to three percent, and from improving the quality of the finish of the reflecting surfaces made it possible to increase the efficiency of the conversion of electric energy into lasing energy to 18 to 20 percent. In addition to an increase in the efficiency of the laser emitter was observed an increase in the unit-length lasing power from eight-to-10 to 30 W/m. The maximum lasing power of the laser reached in the experiments, measured by an IMO-2 receiver, reached 35 W, and the efficiency of the laser emitter equaled 16.5 percent (fig 1). After one hour of operation of the laser, the maximum efficiency was increased to 20 percent, whereby the lasing power equaled 32 W. Then for a few dozen hours the efficiency and lasing power remained unchanged.

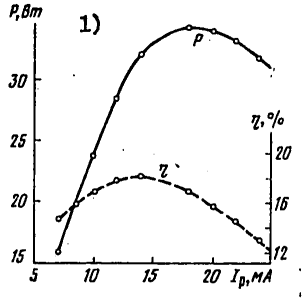

Figure 1. Dependence of Lasing Power, P , and Efficiency of Laser Emitter, η , on Discharge Current, I_r

Key:
1. P , W

It should be mentioned that the temperature of the gas discharge on the axis of the tube, measured by a thermocouple in the absence of lasing, but with discharge parameters optimal for the lasing power, equaled about 420°K (with a unit-length power introduced into the discharge of about 170 W/m). The temperature of the cooling water was then 12 to 14°C.

All the results presented were achieved with an optimal dielectric outlet mirror having a reflection coefficient of 92 percent in the 4 to 7 μ wavelength region.

Estimates have demonstrated that it is possible further to increase the efficiency of a CO laser at room temperature to approximately 25 percent. For this it is necessary to get rid of distortions of the surface of optical elements originating as the result of their compression by the atmosphere and of heating of the outlet mirror on a KCl backing by the laser's radiation.

The necessity of working with dense outlet mirrors, caused by the relatively not too high gain of a CO laser at room temperature, results in a strong growth in power density in the mirror. With a lasing power of about 30 to 32 W and a beam diameter at the outlet mirror of about 8 mm, the density of the incident power at a mirror with optimal transmittance of five to 12 percent equals 0.5 to 1.1 kW/cm^2. With extended operation, distortions of the surface of outlet mirrors become so significant that the lasing power and efficiency of the laser emitter decline substantially. For example, in our experiment after 70 h of operation of an instrument with an outlet mirror having a transmittance of 12 percent, at the maximum lasing power level this power dropped almost twofold. During this period the surface of the mirror was deformed considerably (fig 2). Replacing the working mixture did not result in an increase in lasing power. After the installation of a new outlet mirror the lasing power was restored completely.

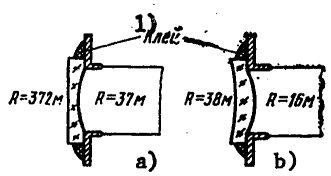

Figure 2. Radii of Curvature of Surfaces of the Outlet Mirror Immediately After Cementing and Evacuation of the Tube (a) and After 70 h of the Laser's Operation (b)

Key:
1. Cement

2. As for the majority of molecular gas lasers, CO_2 for example, lowering of the lasing power and efficiency of a CO laser with an increase in the power of the electric discharge is associated with heating of the gas mixture, whose temperature depends on the conditions for cooling the walls of the gas discharge tube. Therefore it is of practical interest to investigate the influence of the cooling temperature on the energy characteristics of a sealed CO laser. For this purpose the gas discharge tube of the laser described above was filled with a working mixture of $Xe:CO:N_2:He = 1.8:1:3.2:16.5$ with a total pressure of about 24 mm Hg. As the cooling fluid was used antifreeze, which was pumped through in a closed circuit via the heat exchanger and cooling jacket of the gas discharge tube, by means of a fluid pump. The cooling temperature for the gas discharge could be measured within the range of -5 to +40°C. Low temperatures of the antifreeze were achieved by cooling the heat exchanger with vapors of liquid nitrogen, and high by replacing the heat exchanger with a standard thermostat. For the purpose of reducing convective dissipation losses, all elements of the system, including the gas discharge tube, were wrapped with heat insulating asbestos tape. Nevertheless, losses of the thermal loop were great and it was not possible to lower the cooling temperature below -5°C. The temperature of the cooling fluid was measured at the inlet to the laser tube's cooling jacket by means of a thermometer.

Dependences of the efficiency of the laser emitter and of the unit-length lasing power on the temperature of the cooling fluid are shown in fig 3. As is obvious from this figure, with a change in cooling temperature from 40 to 1°C the efficiency increased from 8.5 to 18 percent. Furthermore the unit-length lasing power increased from 13 to 31 W/m. The maximum lasing power at a cooling temperature of 1°C reached 38.5 W, whereby the efficiency equaled 15 percent. Let us note that with this lasing power the density at the outlet mirror with a transmittance of eight percent reached approximately 900 W/cm^2, which resulted in substantial deformation of the mirror's surface.

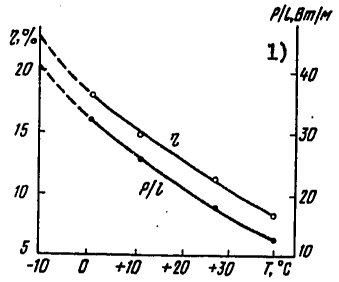

Figure 3. Dependence of the Efficiency, η, and of the Unit-Length Power, P/ℓ, of a Laser Emitter on Temperature of the Cooling Fluid

[Key on following page]

Key:
1. W/m

Estimates made on the basis of the extrapolation in fig 3 demonstrate that by switching to cooling the walls of the gas discharge tubes to the temperature for the condensation of components of the working gas mixture, both the original and those formed in the process of the laser's operation, it is possible to increase the efficiency of sealed CO_2 lasers to at least 35 percent. More intense cooling of the walls of a sealed tube can result in a change in chemical equilibrium in the gas mixture and in limitation of the laser's service life.

As a result of the study made it has been demonstrated that:

1. The efficiency of sealed CO lasers can reach 20 percent with excitation by a self-maintained gas discharge and cooling with water at room temperature.

2. For the purpose of realizing the efficiency reached, as well as for improving it further, it is necessary to improve the quality of the optical elements of the cavity. An increase in the effectiveness of the utilization of cavities of the type of lasers studied can result in an increase in their efficiency to at least 25 percent.

3. For the purpose of eliminating distortions of the surface of mirrors originating because of the high power density (approximately 1 kW/cm^2) striking the outlet mirror, it is advisable to use mirrors on backings made of materials which withstand mechanical and thermal loads without substantial strains.

4. By improving the quality of optical elements and switching to cooling gas discharge tubes with fluids with a reduced temperature (at which freezing of the products of the laser mixture still does not take place) it is possible to achieve an efficiency for sealed CO lasers of approximately 35 percent.

In conclusion the author wishes to express his thanks to V.S. Aleynikov for his useful discussions.

Bibliography

1. Dubrovina, I.V., Ochkin, V.N. and Sobolev, N.N. KVANTOVAYA ELEKTRONIKA, 1, 1851 (1974).

2. Brawne, P.G. and Smith, A.L.S. J. PHYS. E., 8, 870 (1975).

3. Sobolev, N.N. and Sokovikov, V.V. KVANTOVAYA ELEKTRONIKA, edited by N.G. Basov, No 4 (10), 3 (1972).

4. Donnerchache, K.H. EXP. TECH. PHYS., 22, 415 (1974).

CSO: 1862
8831

UDC 621.373.826

EMPLOYMENT OF A TRANSVERSE MICROWAVE DISCHARGE FOR THE PURPOSE OF CREATING A SMALL ECONOMICAL He-Ne LASER

Moscow KVANTOVAYA ELEKTRONIKA in Russian Vol 6 No 10, 1979 pp 2224-2226
manuscript received 18 Dec 78

[Article by Ya.N. Muller, V.M. Geller and V.A. Khrustalev, Electrotechnical Institute, Novosibirsk]

[Text] A study is made of the feasibility of employing a transverse microwave discharge for the purpose of creating a small (active length of 3 to 4 cm) economical He-Ne laser whose pumping source is transistor microwave oscillators. The results are given of an experimental investigation of the energy characteristics of these lasers. It is observed that with an increase in the frequency of the exciting field the laser's output power increases and the required pumping power is reduced, and the degree of localization of the discharge within the limits of the pumping cavity is increased.

An urgent problem at the present time is the creation of small economical He-Ne lasers for utilization in metrology, precision machine building, laser gyroscopy, geodesy, etc. Lasers of this kind with the presence of sufficiently high output power as a rule should be of small weight and size and should have a low noise level, stable ignition of the discharge in the channel, high mechanical strength and durability.

Experience in using different equipment based on He-Ne lasers employing a direct current discharge (RPT) for excitation has disclosed numerous disadvantages of an RPT as a pumping method. Firstly, He-Ne lasers utilizing an RPT have low unit-length gain of the active medium, which makes it necessary to increase their overall size for the purpose of achieving the required output power levels. Secondly, the necessity of using high voltage power sources with special firing equipment hampers the creation of self-contained systems and lengthens the time for lasers to arrive at the working mode. Thirdly, the disintegration of the electrodes reduces the durability of the active element and complicates the technology for its fabrication. In addition, the high noise level worsens the opportunities for using lasers of this kind, especially in measuring systems, and the

presence of reactive parasitic oscillations in the RPT does not make it possible to maintain a stable discharge with low pumping power levels.

The disadvantages enumerated can be eliminated to a considerable extent by employing in these lasers a transverse microwave discharge. In particular, it was demonstrated in [1] that with sufficiently high microwave pumping frequencies stable generation is possible with low values of the laser's active length and of the absorbed microwave power. This makes possible the creation of small economical He-Ne lasers in whose channel a transverse microwave discharge is created and maintained by means of a transistor microwave oscillator.

In the present study are given several results of an investigation of lasers of this type. Glass laser tubes were used, having a channel diameter of 2 mm and a total gas mixture pressure of about 2 mm Hg. The active length of these lasers equaled 3 and 4 cm, and the total length 9 cm. The cavity was formed by outside mirrors with reflection coefficients of 99.9 and 99.7 percent and radii of curvature of 0.5 mm and infinity, respectively. The microwave pumping field was maintained by means of an asymmetric stripline open at the ends of the section, and the conductors of this line adjoined the outside walls of the tube. This section together with a transforming device in the form either of a lumped inductance or of an additional segment of an asymmetric stripline is the collector circuit of the transistor microwave oscillator. This design of the collector circuit made it possible to fire the laser and maintain a steady-state charge by means of one and the same transistor oscillator without any sort of additional regulation and at the same time to eliminate an individual firing device, which is required in He-Ne lasers with a longitudinal discharge. Oscillators of this type were created in the frequency band of 200 to 1000 MHz, based on KT-904A and KT-913B transistors. These oscillators were of the film type on a wafer measuring 20 X 30 X 1 mm. In all experiments was used a direct current source with a voltage of 27 V. The output power of the pumping oscillator could be regulated over a wide range by means of a potentiometer included in the transistor's emitter circuit. In ignition of the discharge in the channel the pumping frequency (operating frequency of the transistor oscillator) was reduced by 1.0 by 1.5 percent.

In fig 1 is shown the dependence of the output power of a laser with an active length of 4 cm in the multimode mode on the microwave power absorbed in the pumping cavity for different pumping frequencies. These results confirm the conclusions made in [1] to the effect that with an increase in pumping frequency the laser power is increased and the required pumping power is reduced considerably. The maximum absolute value of the output power of this laser with an active medium length of 4 cm and a pumping frequency of 900 MHz equals 0.25 mW in the multimode and 0.12 mW in the single-mode mode. In fig 2 are shown the energy characteristics of a laser with an active length of 3 cm (along the X axis is plotted the power required by the transistor pumping oscillator from the direct current source).

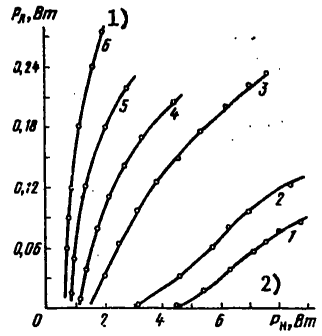

Figure 1. Dependence of Output Power of Laser on Pumping Power for Pumping Frequencies of 470 (1), 540 (2), 675 (3), 800 (4), 900 (5) and 975 (6) MHz

Key:

1. P_1 [laser] , W
2. P_n [pumping] , W

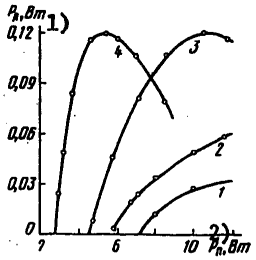

Figure 2. Dependence of Output Power of Laser on the Power Required from the Power Supply by a Transistor Oscillator, for Pumping Frequencies of 500 (1), 700 (2), 875 (3) and 1000 (4) MHz

Key:

1. P_1 , W
2. P_p [power supply] , W

An added advantage of the lasers described is the short time for arriving at the working mode. Investigations conducted have demonstrated that this time, read from the instant the supply voltage is fed to the transistor oscillator, equals 7 to 10 ms. It should be mentioned that with a reduction in pumping power the laser power is reduced monotonically right to the point of the cutoff of generation; furthermore, the steady-state microwave discharge continues to be maintained in the channel, and the radiation intensity of this discharge is also reduced smoothly with a further reduction in pumping power. This testifies to the fact that, unlike lasers with an RPT, in these lasers the active parasitic oscillations are absent [2].

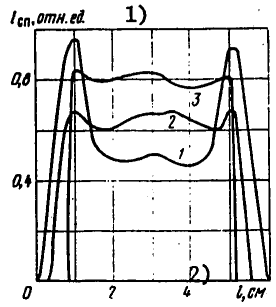

Figure 3. Distribution of Intensity of Secondary Spontaneous Radiation Along the Laser Tube for Pumping Frequencies of 485 (1), 685 (2) and 875 (3) MHz. Ends of the segment of the stripline included in the structure of the pumping cavity measure respectively ℓ = 1 and 5 cm .

Key:

1. I_{sp} [spontaneous] , relative units
2. ℓ , cm

With a short active length of a laser, important is ensuring spatial localization of the plasma, i.e., keeping the plasma within the limits of the pumping cavity and maintaining a high degree of its homogeneity over the length of the channel. Otherwise the stability of the plasma's parameters is reduced, the divergence of the laser emission is increased, and when inside mirrors are used there originates a danger of their breaking. In fig 3 is shown the distribution of the secondary spontaneous radiation measured by means of an interference filter with $\Delta\lambda \approx 3.5$ nm along the length of the tube for different frequencies of the microwave field with a microwave power absorbed in the cavity equal to 4 W. It is obvious from this figure that in the frequency range studied the degree of homogeneity of the plasma and its spatial localization are improved in proportion to an increase in pumping frequency.

Investigations conducted demonstrate the promise of using a transverse microwave discharge for the purpose of creating economical small He-Ne lasers operating in the single-frequency mode. Further improvement of the parameters of these lasers can be related to the employment of inside mirrors, the improvement of the electrodynamic properties of pumping cavities, and a further increase in pumping frequency. Preliminary investigations conducted by us have demonstrated that the power necessary for generation and required by the transistor oscillator from the direct current power supply can be reduced to 2 to 3 W.

Bibliography

1. Muller, Ya.N., Geller, V.M., Lisitsyna, L.I. and Grif, G.I. KVANTOVAYA ELEKTRONIKA, 4, 1788 (1977).

2. Privalov, V.Ye. KVANTOVAYA ELEKTRONIKA, 4, 2085 (1977).

CSO: 1862
8831

UDC 621.373.826

FEATURES OF THE LASER HEATING OF OXIDIZABLE METALS IN AIR WITH OBLIQUE INCIDENCE OF THE RADIATION

Moscow KVANTOVAYA ELEKTRONIKA in Russian Vol 6 No 10, 1979 pp 2232-2236
manuscript received 19 Jun 79

[Article by M.I. Arzuov, A.I. Barchukov, F.V. Bunkin, N.A. Kirichenko, V.I. Konov and B.S. Luk'yanchuk, USSR Academy of Sciences Physics Institute imeni P.N. Lebedev, Moscow]

[Text] A study is made of features of the heating of metals in air with the oblique incidence of continuous laser radiation on the surface of the target. It is demonstrated that with a fixed power there is an optimal angle of incidence of radiation polarized in the incident plane at which heating of the target to a specific temperature is accomplished in a minimal time. With an optimal angle of incidence can be achieved a considerable gain in the expenditure of energy for the laser heating of a number of metals, which has been confirmed by experiments on the angular dependence of the time for the combustion of tungsten.

The laser heating of metals in air is as a rule accompanied by a strong change in the absorbing capacity of targets, associated with the formation of an oxide film on the surface of the metal [1-5]. In [6,7] it was demonstrated that this phenomenon makes it possible considerably to lower the expenditure of energy for heating metals. Moreover, in all the studies enumerated was investigated the case of the normal incidence of radiation on the target. However, as will be demonstrated below, selection of the optimal angle of incidence for the radiation makes it possible to achieve an even greater reduction in energy expenditure (in a number of cases by more than an order of magnitude as compared with the case of normal incidence). This effect is associated with the heavy absorption of radiation polarized in the incident plane at angles close to the Brewster angle.

An experimental investigation was made of the dependence of the time for the combustion, t_v, of a tungsten plate (combustion point of $T_v \simeq 1000°C$) on the angle of incidence, θ, of the unpolarized radiation of a continuous single-mode CO_2 laser with a power of $P = 700$ W. The selection of tungsten as the material for investigation was due to the fact that it oxidizes

quite effectively in air and its combustion is preceded by a strong change in absorbing capacity [8] and the value of t_v practically agrees with the time for activation of the oxidation reaction [5]. The thickness of the plate was $h \sim 0.2$ mm, and the diameter of the radiation spot at $\theta = 0°$ equaled approximately 5 mm and was considerably smaller than the transverse dimensions of the target. The value of t_v was recorded with a stopwatch with a measuring precision of about 1 s. It is obvious from fig 1 that over the entire range of angles θ studied $t_v(\theta)$ is less than $t_v(0)$ (with normal incidence). The minimum of $t_v(\theta)$ is reached with $\theta_{min} \sim 40$ to 60°, whereby t_v at the minimum is approximately 40-fold lower than with $\theta = 0°$.

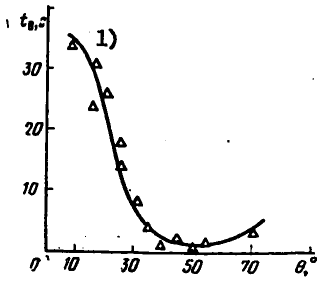

Figure 1. Experimental Angular Dependence of Time for the Combustion of a Tungsten Plate with a Thickness of $h \sim 0.2$ mm. (The diameter of the radiation beam with normal incidence equaled approximately 5 mm and was much smaller than the characteristic transverse dimensions of the plate, $L \sim 5$ cm).

Key:
1. t_v, s

It is known [9] that the absorbing capacity, A, of metals and oxides behaves as a function of the angle of incidence, θ, of the radiation in the following manner: For radiation polarized perpendicularly to the incident plane, $A_\perp(\theta)$ diminishes monotonically with an increase in θ, and for radiation polarized in the incident plane, $A_\parallel(\theta)$ has a maximum with incidence of the radiation at the Brewster angle. The behavior of $A(\theta)$ for pure copper ($x = 0$), pure copper oxide, Cu_2O, and a copper target with an oxide film with a thickness of $x = 3.5$ μ is shown in fig 2. Let us therefore discuss radiation polarized in the incident plane.

When a metal is heated in an oxidative environment by the radiation of a CO_2 laser, the thickness of the oxide film, x, increases with the passage

of time. Accordingly there is a change in the absorbing capacity of the target, $A(x,\theta)$, and in the angle at which absorption is maximum. For function $A(x,\theta)$ can be obtained an approximate expression generalizing for the case of $\theta \neq 0$ the equation obtained in [5]:

$$A(x,\theta) = \cos\theta \frac{n^2 B(\theta)\cos\theta + (2\varkappa n/K)[\beta x - (1 - 2\sin^2\theta/n^2)\sin\beta x]}{n^2\cos^2\theta + [(K^2 - n^4\cos^2\theta)/n^2]\sin^2(\beta x/2)}, \quad (1)$$

where $K = (n^2 - \sin^2\theta)^{1/2}$; $\beta = K4\pi/\lambda$; $B(\theta) = (8A_0\cos\theta)/[(A_0 + 2\cos\theta)^2 + 4\cos^2\theta]$; $\sqrt{\varepsilon} = n + i\varkappa$; ε is the dielectric constant; n and $\varkappa$ are the optical constants of the oxide; and A_0 is the absorbing capacity of the metal with normal incidence of the radiation. Equation (1) is valid with $A_0 << 1$, $\varkappa << 1$, and $\alpha x << 1$ ($\alpha = (4\pi/\lambda)\,\mathrm{Im}\sqrt{\varepsilon - \sin^2\theta}$). These conditions are well fulfilled in heating of the majority of metals by the radiation of a CO_2 laser.

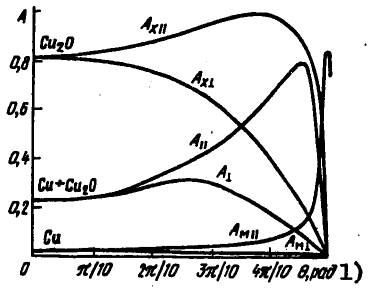

Figure 2. Angular Dependence of the Absorbing Capacity of an Oxide, $Cu_2O(A_x)$, Copper, $Cu(A_m)$, and the Layered System Cu + Cu_2O with an Oxide Film Thickness of $x = 3.5\ \mu$ for Radiation Polarized Perpendicular (Subscript $\perp$) and Parallel (Subscript $\|$) to the Incident Plane.
Note: The Brewster angle of an oxide, θ_κ, in the simplest case of $\kappa = 0$ is determined by the equation $\theta_\kappa = \arccos\ \arccos\,(n^2 + 1)^{-1/2}$ and for a metal, $\theta_m \approx (\pi - {}^{\kappa}A_0/\sqrt{2})/2$.

Key:
1. rad

If the target is thermally delicate, then the rate of its heating is determined by the power, P, of the incident radiation and is described by the equation in [5]:

$$mc\frac{dT}{dt} = PA(x,\theta) - P_{\text{тп}}(T), \tag{2}$$

where m is the mass, c is the specific heat and T is the temperature of the target;

$$P_{\text{тп}}(T)=[\eta(T-T_{\text{н}})+\sigma\sigma_0(T^4-T_{\text{н}}^4)]s \tag{3}$$

is the power of heat losses; s is the area of the surface; and T_n is the original temperature of the target. In (3) the first term describes convective and the second radiative heat losses. Equation (2) is written on the assumption that the target is sufficiently large and the radiation falls entirely onto its surface.

Equations (1) and (2) should be supplemented by the oxidation kinetics equation, which in the majority of cases of practical interest has the form [4,5]

$$\frac{dx}{dt} = \frac{d}{x}\exp\left(-\frac{T_d}{T}\right), \tag{4}$$

where d and T_d are the constants of the parabolic law of oxidation.

The numerical solution with a computer of system of equations (1) to (4) confirms the existence of an optimal angle of incidence of the radiation corresponding to a minimum expenditure of energy. In fig 3 are given angular dependences of the time for heating a copper target to the melting point, $t_{pl}(\theta)$. The minimum on the angular dependence of the time for heating the target with unpolarized radiation is associated with the fact that the increase in term $A_{\parallel}(\theta)$ is considerably greater than the reduction in term $A_{\perp}(\theta)$.

The results of the numerical computation obtained can be illustrated qualitatively in an approximation of the time for activation of the oxidation reaction, t_a, paying attention to the fact that for tungsten $t_a \sim t_{\text{кип}}$, and for metals such as copper, chromium, titanium, etc. $t_a \sim t_{pl}$. A similar approach was used in [6] for determining the optimal power with normal incidence of the radiation on the target and boils down to finding the minimum energy required for activation of the oxidation process.

For small thicknesses of the oxide film ($\beta x \ll 1$) and angles θ not too close to zero or $\pi/2$, from (1) is derived the equation

$$A(x, \theta) = \frac{A_0}{\cos\theta} + \frac{16\pi\kappa}{n^2\lambda}\frac{\sin^2\theta}{\cos\theta}x. \tag{5}$$

Let us consider the case when in (3) only convective heat losses are important. Then, utilizing the results of [10], from (1), (2), (4) and (5), it is possible to obtain the following expression for the time for activation, t_a, of the oxidation reaction:

$$t_a(\theta) = fA_0^4\frac{1}{\cos^2\theta\sin^4\theta}\exp\left(\frac{A_1}{A_0}\cos\theta\right), \tag{6}$$

where

$$f = \frac{4\sqrt{\pi}}{d}\left(\frac{n^2\lambda}{16\pi\kappa A_1}\right)^2, \quad A_1 = \frac{\eta s T_d}{P}.$$

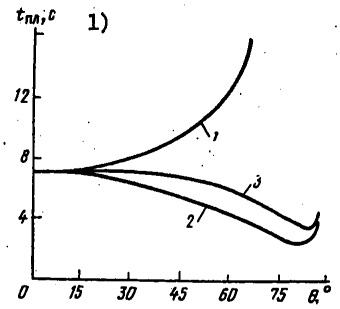

Figure 3. Typical Dependence of Time for Heating a Copper Target in Air to the Melting Point on the Angle of Incidence of the Radiation of a CO_2 Laser Polarized Perpendiculary (1) and Parallel (2) to the Incident Plane, as Well as for Unpolarized Radiation (3). Radiative power $P = 1$ kW ; mass of target $m = 0.7$ g ; area of surface $s = 0.785$ cm^2 ; absorbing capacity of copper $A_0 = 2$ % ; refractive index of oxide, $n = 2.5$; absorption coefficient, $\kappa = 0.02$.

[Key on following page]

Key:
1. t_{pl}, s

From this it is obvious that the activation time, $t_a(\theta)$, has a minimum with an angle value which is determined from the equation

$$\xi \frac{1-\xi^2}{1-3\xi^2} = \frac{2PA_0}{\eta s T_d}, \quad \xi = \cos\theta. \tag{7}$$

From (7) it can be concluded that with an increase in power the optimal value of the angle changes from values close to $\pi/2$ to $\theta = \arccos \arccos (1/\sqrt{3}) \approx 55°$.

In the case when in (3) the key role is played by radiative heat losses, instead of equation (7) for the optimal angle of incidence is obtained the expression

$$\frac{1-\xi^2}{1-9\xi^2}\xi^{1/4} = 2\left(\frac{PA_0}{s\sigma\sigma_0 T_d^4}\right)^{1/4}, \tag{8}$$

where σ is the Stefan-Boltzmann constant and σ_0 is the grayness factor.

The value of the gain in the expenditure of energy for heating the target on account of selection of the optimal angle of incidence can be evaluated by means of the equation

$$\frac{t_a(0)}{t_a(\theta)}\Big|_{\theta=\theta_{opt}} = \frac{4\sqrt{2}\pi^2\varkappa^2}{n^4(n^2-1)A_0^2}\xi(1-\xi^3)(1-3\xi^2)\exp\left[\frac{2(1-3\xi^2)}{\xi(1+\xi)}\right], \quad \xi = \cos\theta_{opt}, \tag{9}$$

where the expression for $t_a(0)$ is obtained in [4,5]. In (9) it is assumed that only convective heat losses are important. It is necessary to keep in mind that equation (9) is valid when the expression in the right half is considerably greater than unity (this is associated with restrictions on values of the angle applied in deriving equation (5)).

It can be concluded from (9) that the energy gain with the oblique incidence of radiation on the target depends heavily on the optical constants of the oxide, n and κ, and for a number of metals, on account of the selection of an optimal angle θ, the ratio $t_a(0)/t_a(\theta)$ can reach values of ~ 10 to 100.

The results obtained above hold true also when taking into account the effects of heat conduction, but acquire certain features. In particular, as it is not difficult to see, in addition to a dependence on the total radiative power, the heating rate begins to depend also on the spatial distribution of the intensity. It must be kept in mind that with oblique incidence the area of the exposed zone increases in proportion to $1/\cos\theta$. Nevertheless it is possible to demonstrate that the intensity, absorbed by a layered system, of radiation polarized in the incident plane has a maximum with oblique incidence, which also explains the experiments on the combustion of tungsten (cf. fig 1). Taking these features into account results in a shift in the minimum of function $t_{p1}(\theta)$ in the direction of smaller angles and in a reduction in the energy gain discussed above.

Let us note in conclusion that the effect of a considerable increase in the heating rate of metals in an oxidative environment with oblique incidence of the radiation can have an important value in technology, in particular in the gas laser cutting of metals.

Bibliography

1. Asmus, J.F. and Baker, F.S. "Rec. 10th Symp. Electron. Ion. Laser Beam Techn.," 1969, p 241.

2. Veyko, V.P., Kotov, G.A., Libenson, M.N. and Nikitin, M.N. DAN SSSR, 208, 587 (1973).

3. Arzuov, M.I., Barchukov, A.I., Bunkin, F.V., Konov, V.I. and Lyubin, A.A. KVANTOVAYA ELEKTRONIKA, 2, 1717 (1975).

4. Arzuov, M.I., Bunkin, F.V., Kirichenko, N.A., Konov, V.I. and Luk'yanchuk, B.S. FIAN Preprint, Moscow, 1978, No 39.

5. Arzuov, M.I., Barchukov, A.I., Bunkin, F.V., Kirichenko, N.A., Konov, V.I. and Luk'yanchuk, B.S. KVANTOVAYA ELEKTRONIKA, 6, 466 (1979).

6. Arzuov, M.I., Bunkin, F.V., Kirichenko, N.A., Konov, V.I. and Luk'yanchuk, B.S. KRATKIYE SOOBSHCHENIYA PO FIZIKE, FIAN, No 11, 43 (1978).

7. Arzuov, M.I., Bunkin, F.V., Kirichenko, N.A., Konov, V.I. and Luk'yanchuk, B.S. PIS'MA V ZHTF, 5, 193 (1979).

8. Arzuov, M.I., Barchukov, A.I., Bunkin, F.V., Konov, V.I. and Luk'yanchuk, B.S. KVANTOVAYA ELEKTRONIKA, 6, 1339 (1979).

9. Landau, L.D. and Lifshits, Ye.M. "Elektrodinamika sploshnykh sred" [Electrodynamics of Continuous Media], Moscow, GITTL, 1957.

10. Libenson, M.N. PIS'MA V ZHTF, 4, 918 (1978).

CSO: 1862
8831

UDC 621.378.325

LIMIT-POWER CHARACTERISTICS OF A NEODYMIUM GLASS LASER IN THE HIGH PULSE REPETITION RATE MODE

Moscow KVANTOVAYA ELEKTRONIKA in Russian Vol 6 No 10, 1979 pp 2245-2248
manuscript received 22 Mar 79

[Article by V.G. Dmitriyev, S.K. Mamonov, O.O. Silichev and A.A. Fomichev, Moscow Physicotechnical Institute]

[Text] A study is made of the power characteristics of a neodymium glass laser near the collapse threshold of the active element (AE). The results are given of calculations of these characteristics for GLS1 and GLS4 glass with different pumping pulse repetition rates (1 to 100 Hz), dimensions and other AE and pumping parameters. By optimization of the laser cavity it was possible to arrive experimentally at lasing power values close to the calculated at frequencies of 20 to 100 Hz.

Solid state neodymium glass lasers are widely used at the present time in the single and widely spaced (with a repetition rate of up to 5 Hz) pumping pulse modes. A higher repetition rate mode (5 to 100 Hz) has been mastered at the present time by lasers employing AIG [expansion unknown]:Nd^{3+}. Neodymium glass lasers, having certain advantages over AIG:Nd^{3+} lasers [1], have in addition substantial disadvantages when operating in the periodic pulse mode. Among these are the worsening of a glass laser's energy parameters with an increase in the pumping pulse repetition rate in the free generation mode [2] and the collapse of the laser's AE under the effect of thermal stresses which originate with sufficiently high mean pumping powers [3]. The latter circumstance imposes a restriction on the maximum achievable mean lasing power, P_g, of a glass laser.

In this paper are given estimates of the magnitude of P_g as a function of the pumping pulse repetition rate, f_n, for several brands of glass, for the purpose of determining the feasibility of creating a glass laser operating in the periodic pulse mode.

The limit output power of a laser is calculated in the following manner. The energy of the heat release, Q, during a single pumping pulse in the laser's AE is proportional to the pumping energy, E_n, absorbed by

neodymium ions: $Q = \sigma_t E_n$, where σ_t is the proportionality factor. When the power of the heat release, $P_t = Qf_n$, reaches a certain maximum value of P^*_t, the AE collapses. Knowing the dimensions, thermophysical and spectroscopic properties of the AE, it is possible to estimate the maximum pumping power absorbed by the AE [3] and the maximum mean lasing power [1] by the equation

$$P_r = \frac{P^*_\tau}{\sigma_\tau} K_z \eta \frac{\nu_r}{\nu_n} \frac{\sqrt{\Phi}-1}{\sqrt{\Phi}} \left(1-\frac{1}{n}\right)\left(1-\frac{\tau}{\tau_n}\ln\frac{n}{n-1}\right), \tag{1}$$

where

$$P^*_\tau = 4\pi l a C \rho \Delta T;\ n = \frac{P^*_\tau}{\sigma_\tau f_n \tau_n P_{\text{пор}}};\quad P_{\text{пор}} = \frac{V h\nu_n \beta \sqrt{\Phi}}{\tau_p \eta_1 \sigma_{32}};$$

$$\Phi = \frac{\tau}{\tau_n} \frac{P^*_\tau}{V\sigma_\tau f_n} \frac{\sigma_{32}}{\beta h\nu_n};$$

$K_z = R_g^2/R_0^2$ is the factor for filling the AE with radiation; η and η_1 are the total quantum yield of luminescence and the quantum yield of luminescence in the 1.06 μ band; ν_g and ν_n are the optical frequencies of generation and pumping; τ_n is the length of the pumping pulse; n_0 is the concentration of neodymium ions; τ is the lifetime; τ_r is the radiative lifetime of the metastable level (at a wavelength of 1.06 μ); σ_{32} is the transverse cross section of the forced transition; β represents losses normalized for double the length of the AE; V, l, and R_0 are the volume, length and radius of the AE, respectively; a, C and ρ are the heat conduction, specific heat and density of the AE's material; ΔT is the thermostability of the AE. When the temperature drop between the center and side surface of the AE is not too high, i.e., it is possible to disregard spherical aberrations of the AE's thermal lens caused by the dependence of thermal optical constants P and Q on temperature [4], the value of σ_t is determined from the experimental dependence of the strength of the thermal lens of the AE ($1/f_t$) on the pumping power supplied to the tube, P_n,

$$1/f_t = l\,(P-Q/2)\sigma_T \sigma_0 P_n/(2\lambda), \tag{2}$$

where σ_0 is the efficiency of the light source and λ is the heat conduction coefficient. The value of σ_0 can be estimated by the procedure described in [1]; other parameters of the problem are taken from [5].

On the basis of the dependence of diffraction losses of modes of different orders on the Fresnel number for the case of a confocal cavity [6], it is

possible to make a rough estimate of the value of the filling factor, $K_z \approx 0.6 - (\omega_0/R_0)^2$, where ω_0 is the amount of constriction of the fundamental mode in the AE. This estimate is valid in the case when in the transverse section the laser's radiation has a regular mode structure, i.e., only with a sufficiently uniform distribution of gain over the model's cross section.

In fig 1 are shown the results of a computation of P_g by equation (1) for an AE made of GLS1 and GLS4 glass with different values of f_n.

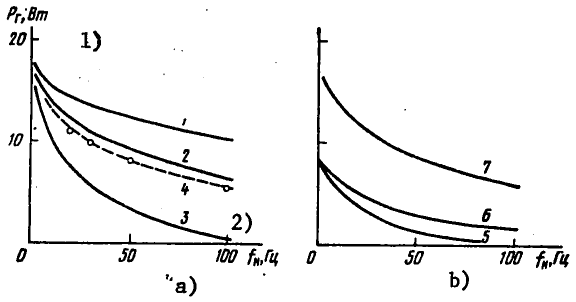

Figure 1. Dependence of the Limit Lasing Power of a Neodymium Glass Laser on the Pumping Pulse Repetition Rate for GLS1 (a) and GLS4 (b) Glass: $\ell = 5$ cm ; $\eta = 0.75$ (a) and 0.5 (b) ; $\sigma_t = 0.65$ (a) and 0.6 (b) ; $\beta = 0.002$ (1 to 4, 6, 7) and 0.004 cm^{-1} (5); $K_z = 0.5$; 1--$R_0 = 0.15$; 2 and 4 to 7--$R_0 = 0.25$; 3--$R_0 = 0.5$ cm ; 4--experiment; 7--AE reinforced (ΔT increased twofold)

Key:
1. P_g, W
2. f_n, Hz

In the table are given values of P^*_t for different grades of glass (AE 5 cm long), which can be used for determining the promise of using a specific grade of glass in the periodic pulse mode. Not taken into account in the calculations is the change in losses and filling factor, K_z, with an increase in pumping power, caused by distortion of the cavity by the AE's thermal lens [2] and resulting in a drop, characteristic of a neodymium glass laser, in output energy with an increase in f_n while maintaining the pumping energy (fig 2, curve 1). Experiments have shown that with the employment of a diffuse light source, when the AE's thermal lens is described well by an approximation of a thick lens, the main reason for this drop is induced birefringence in the AE. The influence of the latter is stronger, the greater the constriction of the fundamental mode, ω_0,

in the AE, i.e., the greater the scale of individual elements of the mode structure. A reduction in ω_0 results in an increase in the number of modes generated and in a substantial improvement in the laser's energy parameters at high pumping pulse repetition rates. For example, a reduction of ω_0 from 0.6 to 0.3 mm results in considerable leveling of the frequency generation characteristic (cf. fig 2, curve 2) right up to frequencies at which the collapse of the AE takes place (approximately 100 Hz). Thus, in an experiment it is possible to realize conditions sufficiently close to those under which a calculation was made of limit characteristics.

Table

Brand of glass		P^*_t, W
Silicate	GLS1	58
	GLS4	39
	LGS236-2	33
Phosphate	LGS55	16
	LGS56	13
	LGSI2	12

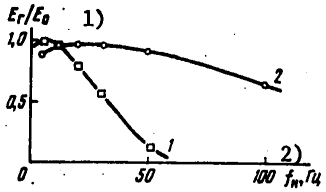

Figure 2. Experimental Dependence of the Lasing Energy of a Laser with an AE Made of GLS1 Glass Measuring ∅5 X 50 mm and a Diffuse Light Source, on the Pumping Pulse Repetition Rate with E_n = 20 J (with f_n = 50 Hz, $\omega_0 \approx 0.6$ (1) and 0.3 mm (2); E_0 = 0.05 J)

Key:
1. E_g/E_0
2. f_n, Hz

In conducting experiments for determining P_g (for the case of an AE made of GLS1) a diffuse light source was used, and a cavity with high pumping power made possible a constriction of approximately 0.3 mm. The magnitude

of P_g was determined with a constant value of f_n and with a gradual increase in pumping energy in the pulse to the point of collapse of the AE. The transmission coefficient of the outlet mirror equaled the optimal. Each experimental point (cf. fig 1a) represents a value averaged for several models, since the thermal strength of the AE has a fairly wide variance [5]. It is obvious that the experimental results agree sufficiently well with the calculations presented.

It should, of course, be expected that reinforcement of the AE (tempering [7], etching of the side surface, etc.) should result in an increase in P^*_t and P_g. Thus, reinforcement of the AE (e.g., increasing ΔT twofold) results in a considerable increase in the limit lasing power at high pumping pulse repetition rates (cf. fig 1b).

In conclusion the authors wish to use this occasion to express their gratitude to M.F. Stel'makh for his useful discussions.

Bibliography

1. Stepanov, B.I., ed. "Metody rascheta opticheskikh kvantovykh generatorov" [Methods of Calculating Lasers], Minsk, Nauka i Tekhnika, 1966, 1968.

2. Mak, A.A., Soms, L.N., Stepanov, A.I. and Sudakov, A.B. OPTIKA I SPEKTROSKOPIYA, 30, 1081 (1971).

3. Belostotskiy, B.R. and Rubanov, A.S. "Teplovoy rezhim tverdotel'nykh opticheskikh kvantovykh generatorov" [Thermal Conditions of Solid State Lasers], Moscow, Energiya, 1973.

4. Alekseyev, N.Ye., Gromov, A.K., Izyneyev, A.A., Kopylov, Yu.L. and Kravchenko, V.B. KVANTOVAYA ELEKTRONIKA, 6, 140 (1979).

5. Avakyants, L.I., Buzhinskiy, I.M., Koryagina, Ye.I. and Surkova, V.F. KVANTOVAYA ELEKTRONIKA, 4, 120 (1978).

6. Vaynshteyn, L.A. "Otkrytyye rezonatory i otkrytyye volnovody" [Open Cavities and Open Waveguides], Moscow, Sovetskoye Radio, 1966.

7. Mak, A.A., Mit'kin, V.M., Polukhin, V.I., Stepanov, A.I. and Shchavelev, O.S. KVANTOVAYA ELEKTRONIKA, 2, 850 (1975).

CSO: 1862
8831

END